

Nuclear Electric Quadrupole Interactions in Crystals*

R. V. POUND

Harvard University, Cambridge, Massachusetts

(Received April 3, 1950)

A study is made of the effects of the presence of nuclear electric quadrupole moments on the nuclear magnetic resonance absorption in solids. Necessary theoretical background is followed by descriptions of experiments in which the spectra obtained with an r-f spectrograph, described elsewhere, are found to show marked splitting resulting from the quadrupole interaction with the electric field gradient. Both powder patterns and spectra of single crystals are reported, for Li^7 , Na^{23} , and Al^{27} , with splittings varying from about 20 kc to 718 kc, depending on the crystal and the nucleus. Unambiguous indication of the spin values is obtained. The possibility of the detection of a resonance resulting from the electric quadrupole splittings in the absence of a static magnetic field is discussed and an unsuccessful attempt to find such a resonance in ICl is described and the failure tentatively explained. Available signal-to-noise ratios are calculated for such

resonances. A method is described of determining the frequency of a large electric quadrupole splitting, by observation of the dependence of the frequency of the magnetic splitting of the levels $m = \pm \frac{1}{2}$, for an odd half-integral spin, on the angle between the direction of a magnetic field and the symmetry axis of the crystalline field. The electric quadrupole moment is shown probably to account for relaxation times of nuclei of spin greater than $\frac{1}{2}$ even in cubic crystals and, as evidence, resonances of Na^{23} , Li^7 , I^{127} , and Br^{81} are reported. Assuming partial saturation and electric quadrupolar relaxation, calculations are made to account for a departure of the intensity ratios of the lines, in the Na^{23} spectrum in NaNO_3 , from the ratios of the transition probabilities for magnetic dipole radiation. The possibility of determining nuclear electric quadrupole moments from splittings or relaxation times in ionic crystals is discussed.

I. INTRODUCTION

NUCLEAR paramagnetic resonance¹ or nuclear induction² provides means of observing the interactions between atomic nuclei and their surroundings. Such interactions affect relaxation times,^{3, 4} line widths,^{3, 5} and frequencies,^{6, 7} and in some cases can be the cause of the splittings of otherwise single lines into multiple ones.⁸⁻¹⁰ The principal kinds of interactions of which studies have been reported are of magnetic character. The large majority of careful investigations of these aspects of the effect has involved the proton resonance, except in the experiments dealing only with determining nuclear g -factors, and because the proton spin is only $\frac{1}{2}$, no interactions of electric origin could be expected.

Many determinations of g -factors of nuclei of higher spin have been made in aqueous solutions or liquids, and it is common in these to find a resonance line that is considerably broader than a proton line in water and which cannot be saturated easily, indicating a correspondingly short relaxation time.^{11, 12} This observation has been explained as the effect of the interaction between the nuclear electric quadrupole moment and the gradient of the electric field at the nucleus. Because of the short time, compared with the period of the

resonance frequency, in which a local configuration in the liquid changes character, no line structure is contributed by this interaction, the average value of the perturbation over the lifetimes of the nuclear spin orientation being zero. It is a strong mechanism for thermal relaxation, however, and becomes the dominant mechanism for even the deuteron, with the smallest known non-zero quadrupole moment, in D_2O . Unfortunately, the motion in the liquid, especially in concentrated ionic solutions, is so complex that observation of the broadening or of the relaxation effect does not allow a very accurate estimate of the magnitude of the quadrupole interaction. It has been used for rough determinations of the ratios of quadrupole moments of isotopes, however. The two g -factors of the two naturally equally abundant bromine isotopes were assigned by correlating the observed line breadths with the known quadrupole moments.¹¹

That the quadrupole interaction can be the dominating relaxation mechanism in the fluctuating liquid system even for the deuteron, indicates that in the solid state one must expect to find line shapes determined predominantly by the electric quadrupole interaction, if it exists. Indeed, it must also be the dominant factor in the thermal relaxation process in the absence of electronically paramagnetic ions or impurities, if one considers a theory along the lines of Waller.¹³ Both of these expectations appear to be verified experimentally, in some cases, as will be shown.

II. THEORY

The energy of interaction between a nucleus and a surrounding charge distribution can be written as an expansion in Legendre polynomials as

$$V = \sum_{i,j} (e_i e_j) / r_{ij} = \sum_{i,j} (e_i e_j / r_j) \sum_{k=0}^{\infty} (r_i / r_j)^k P_k(\cos \theta_{ij}), \quad (1)$$

* Some of the results presented here have been reported briefly previously. R. V. Pound, *Phys. Rev.* **73**, 1247 (1948); R. V. Pound, *Proc. Phys. Soc.* **61**, 576 (1948).

¹ Purcell, Torrey, and Pound, *Phys. Rev.* **69**, 37 (1946).

² Bloch, Hansen, and Packard, *Phys. Rev.* **70**, 474 (1946).

³ Bloembergen, Purcell, and Pound, *Phys. Rev.* **73**, 679 (1948).

⁴ N. Bloembergen, Thesis, Leiden (1948).

⁵ Purcell, Bloembergen, and Pound, *Phys. Rev.* **70**, 988 (1946).

⁶ W. D. Knight, *Phys. Rev.* **76**, 1259 (1949).

⁷ W. G. Proctor and F. C. Yu, *Phys. Rev.* **77**, 717 (1950); W. C. Dickinson, *Phys. Rev.* **77**, 736 (1950).

⁸ G. E. Pake, *J. Chem. Phys.* **16**, 327 (1948).

⁹ N. Bloembergen, *Physica* (to be published); private communication.

¹⁰ Gutowsky, Kistiakowsky, Pake, and Purcell, *J. Chem. Phys.* **77**, 972 (1949).

¹¹ R. V. Pound, *Phys. Rev.* **72**, 1273 (1948).

¹² R. V. Pound, *Phys. Rev.* **73**, 1112 (1948).

¹³ I. Waller, *Zeits. f. Physik* **79**, 370 (1932).

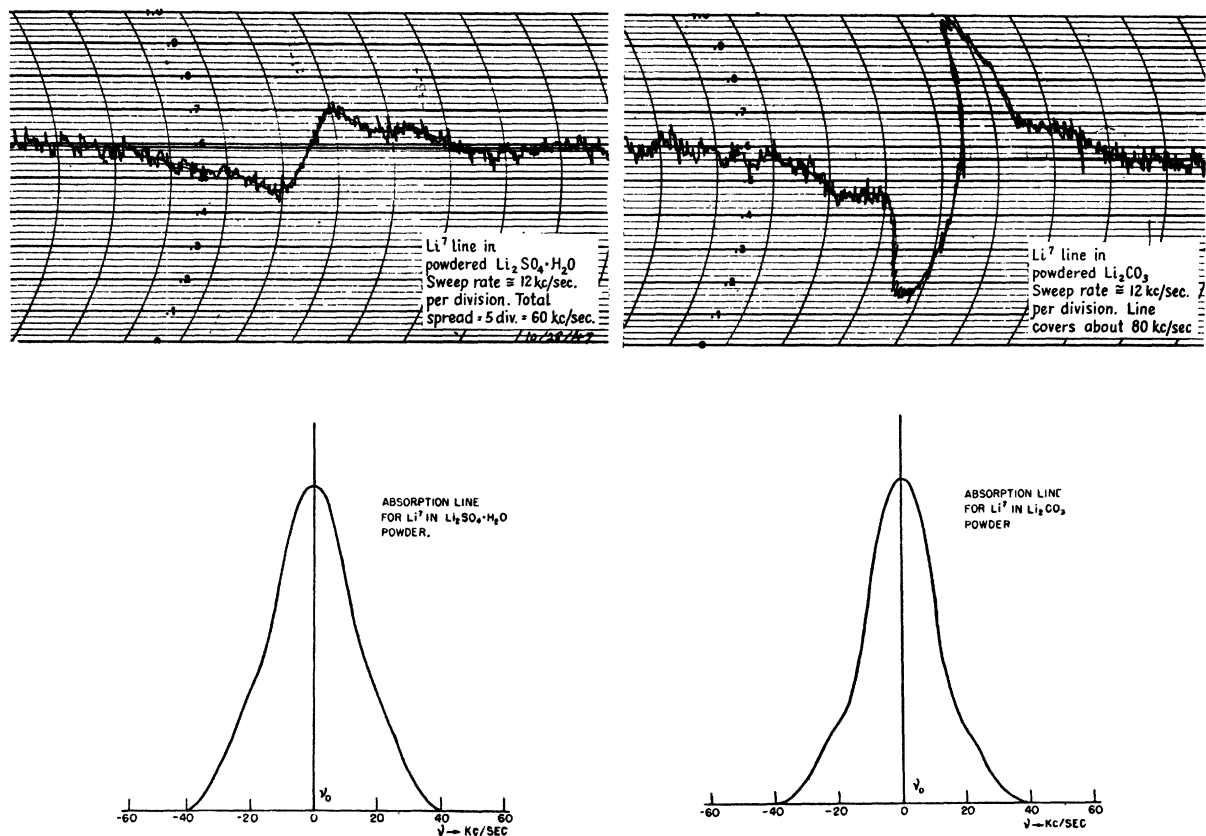


FIG. 1. Records of Li^7 resonance near 3 Mc in powdered $\text{Li}_2\text{SO}_4 \cdot \text{H}_2\text{O}$, at left, and Li_2CO_3 , at right. Below are absorption curves obtained from assuming records are derivatives.

where e_i refers to an element of the nuclear charge, e_j to an external charge, r_i and r_j the distances from the origin, taken at the center of the nucleus, to the charges e_i and e_j , respectively, and θ_{ij} is the angle between these radius vectors. By the addition theorem of spherical harmonics, we can express the interaction in terms of θ_i , ϕ_i , θ_j , and ϕ_j the polar and azimuthal angles between the z axis, the xz plane, and r_i and r_j . Thus (1) becomes

$$V = \sum_{k=0}^{\infty} (e_i e_j / r_j) \sum_{q=-k}^k (r_i / r_j)^k \sum_{q=-k}^k (-)^q (4\pi / 2k + 1) \times Y_k^{-q}(\cos\theta_i, \phi_i) Y_k^q(\cos\theta_j, \phi_j), \quad (2)$$

where $Y_k^q(\cos\theta, \phi)$ is the normalized tesseral harmonic

$$Y_k^q(\cos\theta, \phi) = \Theta_k^q(\cos\theta) \epsilon^{iq\phi} / (2\pi)^{1/2} \quad (3)$$

and the functions $\Theta_k^q(\cos\theta)$ are defined¹⁴ as

$$\Theta_k^q(\cos\theta) = (-)^q [(2k+1)(k-q)! / 2(k+q)!]^{1/2} \times \sin^q \theta \frac{d^q}{(d \cos\theta)^q} P_k(\cos\theta) \quad (4)$$

¹⁴ E. U. Condon and G. H. Shortley, *The Theory of Atomic Spectra* (Cambridge University Press, London, 1935).

for $q > 0$, with

$$\Theta_k^q(\cos\theta) = (1)^q \Theta_k^{-q}. \quad (5)$$

In this manner the interaction can be written as

$$V = \sum_{i,j} (e_i e_j / r_j) \sum_{k=0}^{\infty} (r_i / r_j)^k [C^{(k)}(i) \cdot C^{(k)}(j)], \quad (6)$$

where $C^{(k)}(i) \cdot C^{(k)}(j)$ is the tensor scalar product defined as

$$\sum_{q=-k}^k (-)^q C_q^{(k)}(i) C_{-q}^{(k)}(j) \quad (7)$$

and¹⁵

$$C_q^k = [4\pi / (2k+1)]^{1/2} Y_k^q(\cos\theta, \phi). \quad (8)$$

We are concerned with the electric quadrupole term in the interaction which involves the tesseral harmonics of order $k=2$, the lowest order to be non-zero. Thus the interaction can be written as the dyadic product

$$F = \mathbf{Q} \cdot \nabla \mathbf{E},$$

where

$$\mathbf{Q} = \sum_i e_i r_i^2 C^{(2)}(i) \quad (9)$$

¹⁵ G. Racah, *Phys. Rev.* **62**, 438 (1942).

and

$$\nabla\mathbf{E} = \sum_j (e_j/r_j^3) C^{(2)}(j). \quad (10)$$

From the symmetry properties of the nucleus, the interaction will vanish unless the spin $I \geq k/2$ and k is even, which, for the quadrupole interaction $k=2$, requires $I \geq 1$.

This formulation of the interaction expresses both the tensors of the nuclear charge and of the external charge as irreducible representations of the three-dimensional rotation group.¹⁶ That at most five independent components are required to determine the tensor can be understood through the consideration of the tensor expressed in rectangular coordinates, which has nine components. However, the requirement that it be symmetric and that it be traceless, since $\nabla \cdot \mathbf{E} = 0$, reduces these to five independent components. The definition of $(\nabla E)_0$, above, can be used to express the irreducible tensor components from the components of the rectangular coordinate system, since

$$(\nabla E)_0 = \frac{1}{2}(\partial E_z/\partial z) = \frac{1}{3}[\frac{2}{3}(\partial E_z/\partial z) - \frac{1}{2}\nabla \cdot \mathbf{E}]. \quad (11)$$

The other components may be derived from this by the same method as that employed to derive the tesseral harmonics from the Legendre polynomials, and one obtains

$$\left. \begin{aligned} (\nabla E)_0 &= -\frac{1}{2}(\partial E_z/\partial z), \\ (\nabla E)_{\pm 1} &= \pm (6^{1/2}/6)[(\partial E_x/\partial z) \pm i(\partial E_y/\partial z)], \\ (\nabla E)_{\pm 2} &= - (6^{1/2}/6)[(\partial E_x/\partial x) - (\partial E_y/\partial y) \\ &\quad \pm 2i(\partial E_x/\partial y)]. \end{aligned} \right\} (12)$$

These are analogous to the five components of the nuclear electric quadrupole moment operator derived in a similar manner

$$\left. \begin{aligned} Q_0 &= [eQ/2I(2I-1)][3I_z^2 - I(I+1)], \\ Q_{\pm 1} &= \mp (6^{1/2}/2)[eQ/2I(2I-1)][(I_x + iI_y)I_z \\ &\quad + I_z(I_x + iI_y)], \\ Q_{\pm 2} &= (6^{1/2}/2)[eQ/2I(2I-1)][(I_x + iI_y)^2], \end{aligned} \right\} (13)$$

where the scalar nuclear quadrupole moment Q is defined in the conventional manner^{17,18}

$$eQ = (II) \left| \sum_i e r_i^2 (3 \cos^2 \theta_{iI} - 1) \right| (II). \quad (14)$$

The non-vanishing matrix elements of the electric quadrupole tensor

$$F = \mathbf{Q} \cdot \nabla \mathbf{E} = \sum_{q=-2}^2 (-1)^q Q_q (\nabla E)_{-q}, \quad (15)$$

in an I, m representation involve only the well-known matrix elements of the angular momentum and can be

written down at once.

$$\left. \begin{aligned} \langle m | F | m \rangle &= A[(3m^2 - I(I+1))(\nabla E)_0], \\ \langle m | F | m \pm 1 \rangle &= \mp (6^{1/2}/2)A(2m \pm 1) \\ &\quad \times [(I \pm m + 1)(I \mp m)]^{1/2}(\nabla E)_{\pm 1}, \\ \langle m | F | m \pm 2 \rangle &= (6^{1/2}/2)A[(I \mp m)(I \mp m - 1) \\ &\quad \times (I \pm m + 1)(I \pm m + 2)]^{1/2}(\nabla E)_{\pm 2}, \end{aligned} \right\} (16)$$

where $A = eQ/2I(2I-1)$. Comparison of these matrix elements with those calculated for the interaction in diatomic molecules^{18,19} reveals that the present problem could be treated as the limiting case of that system, regarding J as tending toward infinity, in which case $m_J/J \rightarrow \cos \theta$, $[1 - (m_J/J)^2]^{1/2} \rightarrow \sin \theta$ and the ϕ dependence averages out because of the precession of J about the z -direction. The present treatment has greater utility in that it allows the evaluation of the matrix elements for cases of other than axial symmetry. For axial symmetry, as in diatomic molecules, the five components $(\nabla E)_q$ can be expressed in terms of a single scalar,

$$eq = \sum_j e_j (3 \cos^2 \theta_j - 1) r_j^{-3}, \quad (17)$$

where θ_j is the angle between \mathbf{r}_j and the symmetry axis. For axial symmetry the components of the tensor $\nabla \mathbf{E}$ are

$$\left. \begin{aligned} (\nabla E)_0 &= \frac{1}{4}eq(3 \cos^2 \theta - 1), \\ (\nabla E)_{\pm 1} &= \pm \frac{1}{4}6^{1/2}eq \sin \theta \cos \theta \epsilon^{\pm i\phi}, \\ (\nabla E)_{\pm 2} &= \frac{1}{8}6^{1/2}eq \sin^2 \theta \epsilon^{\pm 2i\phi}, \end{aligned} \right\} (18)$$

where θ is the angle between the axis of symmetry and the z direction and ϕ is the angle between the projection of the axis of symmetry on the x, y plane and the positive x -direction. For lower than axial symmetry one needs to know the three mutually perpendicular principal axes of the tensor in which the 3×3 matrix of the rectangular components of $\nabla \mathbf{E}$ is diagonalized. If the z -axis is chosen along the principal axis having largest component, then $(\nabla E)_0 = eq/2$ where q is defined as before, $(\nabla E)_{\pm 1} = 0$ and $(\nabla E)_{\pm 2} = (3^{1/2}/6)\eta eq$ where $\eta = (\partial E_x/\partial x - \partial E_y/\partial y)/(\partial E_z/\partial z)$ and by definition

$$0 \leq |\eta| \leq 1.$$

III. EXPERIMENTAL TECHNIQUE

The foregoing theory will be developed as it applies to the experiments, carried out and contemplated, con-

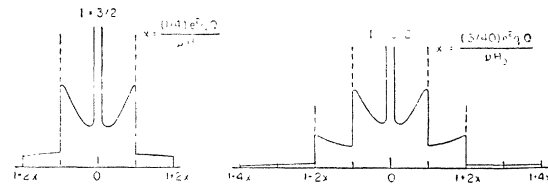


Fig. 2. Calculated absorption curves for $I=3/2$ and $I=5/2$ in powdered samples, ignoring broadening from magnetic dipole interactions.

¹⁶ E. Wigner, *Gruppentheorie*, etc. (Friedr. Vieweg, Braunschweig, 1931), reprinted by J. W. Edwards, Ann Arbor.

¹⁷ H. B. G. Casimir, *On The Interaction Between Atomic Nuclei and Electrons* (De Erven F. Bohn N.V., Haarlem, 1936).

¹⁸ B. Feld and W. E. Lamb, *Phys. Rev.* **67**, 15 (1945).

¹⁹ Kellogg, Rabi, Ramsey, and Zacharias, *Phys. Rev.* **57**, 677 (1940).

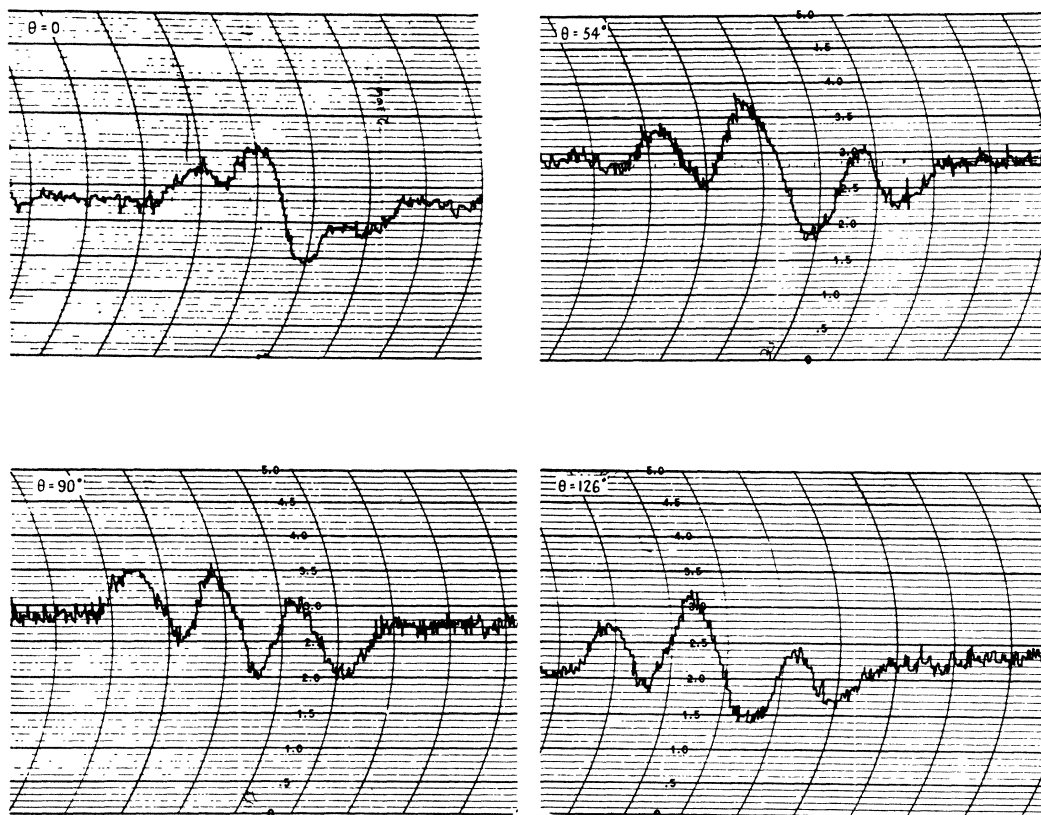


FIG. 3. Recorded resonances of Li^7 in single crystal of $\text{Li}_2\text{SO}_4 \cdot \text{H}_2\text{O}$, for various values of θ , the angle between the c axis and H_0 , with H_0 in the bc plane. The frequency scale is about 12 kc per division.

currently with the description of the experiments. The apparatus used for most of the experiments was the recording r-f spectrograph described elsewhere^{20, 21} which has several properties recommending it for investigations of this type. It responds almost uniquely to the absorption part of the nuclear resonance effect. In contrast, bridge circuits¹⁻³ respond either to the absorption or the dispersion or a mixture of the two, depending on the phase of the residual unbalance signal, which is difficult to maintain constant over long periods of time. The frequency is easily slowly swept continuously over a range as large as 2.5 to 1, at any radiofrequency in the range from 45 Mc downward. The lowest frequency so far tried is 350 kc. The recording milliammeter gives permanent records approximating derivatives of absorption lines with respect to the magnetic field or the frequency, because the magnetic field is modulated sinusoidally with a peak-to-peak swing less than the line-breadth. A rough frequency calibration is provided by the time scale on the records, which correlates with the frequency control of the oscillator. The frequency control is driven by a synchronous motor geared down to a rate ranging from one revolution (two sweeps) in ten hours down to one revolution in ten days.

²⁰ R. V. Pound, Phys. Rev. **72**, 527 (1947).

²¹ R. V. Pound and W. D. Knight, Rev. Sci. Inst. **21**, 219 (1950).

The earlier experiments were performed with an electromagnet with poles $3\frac{1}{2}$ in. in diameter and a $1\frac{1}{2}$ in. gap, a modulation frequency near 1300 c.p.s., and samples $\frac{1}{2}$ in. diameter by $\frac{1}{2}$ in. long. The magnet was supplied from large storage batteries and was operated continuously, day and night. Many line strengths were such that the 20-sec. time constant, or 0.05 c.p.s. band width had to be used in the recording system and this set an upper limit on the sweep rate that could be used to get full detail in line shapes. Usually a sweep from 4 to 2 Mc in 3 days was used with a straight-line-capacity condenser determining the frequency. Therefore the rate of change of frequency was highest at the high frequency end of the sweep. The magnetic field required for such nuclei as Na^{23} , Br^{79} , Br^{81} , Li^7 , and Al^{27} for this range was between 1200 and 2500 gauss and the inhomogeneity of the field of less than 2 gauss over the sample was not a serious handicap because the line-breadth caused by dipole-dipole broadening was usually of this order or larger.

A slow drift of the field made precision measurements of frequency differences difficult, however, and, rather than attempt to control the field for the continuous operation, a permanent magnet was constructed with which the later experiments were performed. This has a gap of 6 in. diameter, $1\frac{3}{8}$ in. spacing, supplied with a

field of 6379 gauss from about 350 lb of Alnico V. The field appears to be homogeneous to better than 0.1 gauss over the same $\frac{1}{2}$ in. diameter samples, and is considerably more homogeneous over $\frac{1}{4}$ in. diameter samples. No long time drift of the field has so far been observed (about six months since first used, one year since originally magnetized to saturation without the conventional small demagnetization for stabilization). There did appear to be a decrease by about 4 gauss during the summer months when the laboratory was excessively hot. This loss of field was regained when the laboratory temperature returned to normal, and could have been caused by a differential thermal expansion effect.

Modulation of the field is achieved in the magnet by a pair of small coils in the gap itself. A modulation frequency of about 280 c.p.s. is used. When frequency differences and ratios were measured, a Navy type LM-18 frequency meter was used and the current in the electromagnet was monitored with a potentiometer and drift corrected as required. Since many hours were consumed in a single set of measurements in some cases, this became very tedious and the permanent magnet has helped greatly in simplifying the procedure and improving the precision obtainable.

IV. RESULTS AND THEORY

Several different kinds of spectra have been found so far and these will be discussed below, classified according to the nucleus of which the magnetic resonance was observed.

Lithium

The resonance of only the Li^7 isotope has so far been detected in the crystalline state. The first samples used were pellets of $Li_2SO_4 \cdot H_2O$ and of Li_2CO_3 compressed

from a powder. The resulting records are shown in Fig. 1 together with absorption curves derived from these by numerical integration. That these lines show some evidence of structure is clearer from the recorded derivatives than from the integrals. The width of the Li_2CO_3 line is about 60 kc between the outer ends of the initial and final flats in the record, and this is an order of magnitude greater than would be possible from dipole-dipole broadening, being equivalent to a local field of about ± 18 gauss.

To interpret this line as due to the quadrupole interaction, the first-order perturbation on the energies of the levels m in the magnetic field may be calculated. This is simply

$$E_m = (m\mu H/I) + [eQ/2I(2I-1)][3m^2 - I(I+1)](\nabla E)_0. \tag{19}$$

In this case, since the sample is really a powder, a uniform distribution of the direction of the crystalline axes with respect to the magnetic field direction exists and therefore a corresponding distribution of the magnitude of $(\nabla E)_0$. To solve this problem properly one should know the field symmetry at the nucleus but the lines are not well enough resolved to be significantly affected by such symmetry, and an assumption of axial symmetry may be made. With this assumption, $(\nabla E)_0 = \frac{1}{4}eq(3 \cos^2\theta - 1)$ and with a uniform distribution in space of the orientations of the crystalline axes one would expect the line corresponding to $E_{\frac{3}{2}} - E_{-\frac{3}{2}}$ to be at the frequency corresponding to the normal gyromagnetic ratio for Li^7 , but the transitions corresponding to $E_{\frac{3}{2}} - E_{\frac{1}{2}}$ and to $E_{-\frac{1}{2}} - E_{-\frac{3}{2}}$ to produce absorption over the ranges, relative to the normal frequency, from $\pm e^2Qq/2h$ to $\mp e^2Qq/4h$, respectively. The resulting shape function for the line is identical to that computed for heteronuclear diatomic molecules of a large J value

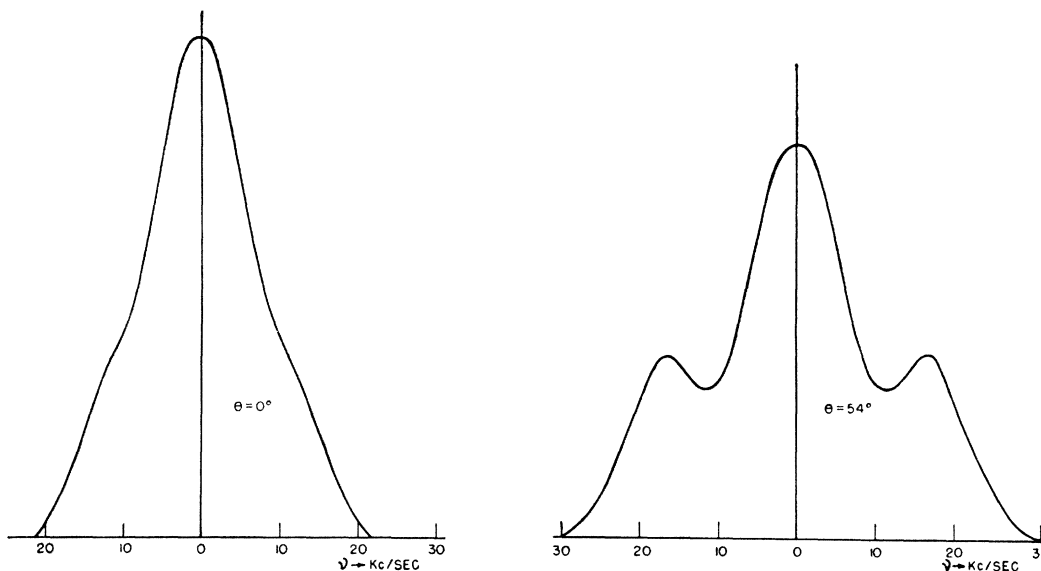


FIG. 4. Absorption curves for the Li^7 line from Fig. 3 for $\theta = 0^\circ$, at left, and $\theta = 54^\circ$, at right.

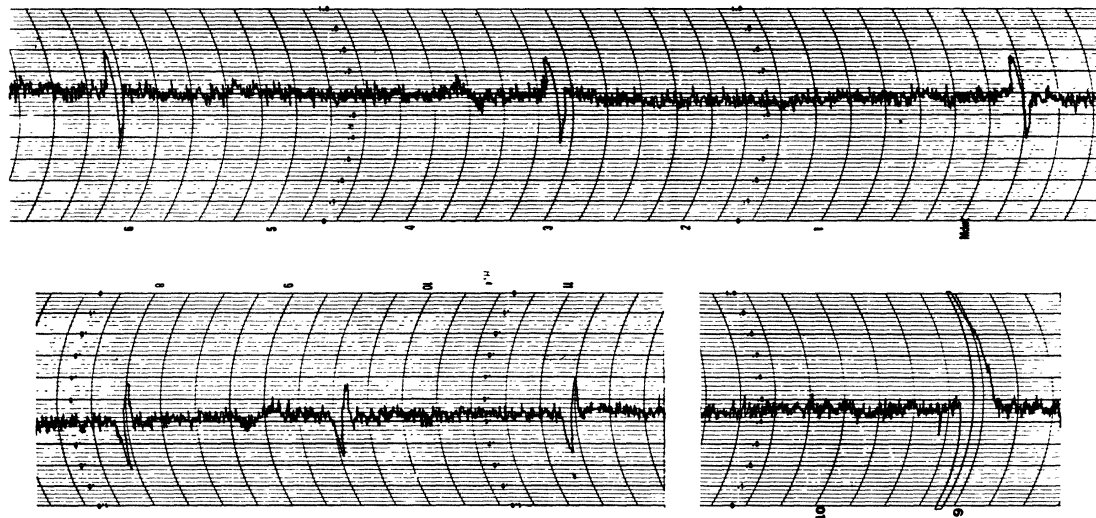


FIG. 5. The Na^{23} resonance in NaNO_3 for crystal axis near 0° , 90° , and 54° with respect to H_0 . The frequency scale is about 14 kc per division, which corresponds to 15 minutes of time. The frequency of the center line is 7.18 Mc. A small effect explainable through higher order terms in the perturbation can be seen to cause an asymmetry in the line at $\theta = 54^\circ$.

by Feld and Lamb,¹⁸ and the arguments given there will not be repeated here. Resulting curves of line intensity for the above case of $I = \frac{3}{2}$ and for the similar situation with $I = 5/2$ are reproduced in Fig. 2.

The magnetic dipole interaction has been ignored in the computation of these shapes and if the broadening from this cause is not negligible compared to e^2qQ , the irregular shape would be considerably smoothed out. In addition, there is the possibility that all Li^7 nuclei are not similarly situated, and in that event several such lines with several values of q might be superimposed. Thus very little information is obtained from a spectrum of this type beyond the evidence that a quadrupole interaction seems to be required to account for the breadth.

A single crystal of $\text{Li}_2\text{SO}_4 \cdot \text{H}_2\text{O}$ was obtained^{21a} and the required $\frac{1}{2}$ -in. diameter sample cut with its axis normal to the b, c plane of the monoclinic structure. The spectra obtained for several orientations of this crystal in the magnetic field, where the indicated angle θ is the angle between the magnetic field direction and the c axis of the crystal, are shown in Fig. 3. The splitting here is much more distinct and shows a definite triplet structure with a maximum splitting near $\theta = \pm 54^\circ$ and $\pm 126^\circ$, and minimum at 0° and 180° . Curves at the absorption obtained by numerical integration of the spectra for the maximum and minimum splitting, plotted against a frequency scale in kc/sec. relative to the center are shown in Fig. 4. The maximum separation between the satellites is 45 kc.

An attempt to account for the angular dependence of the splitting in terms of the $\text{Li}_2\text{SO}_4 \cdot \text{H}_2\text{O}$ crystal struc-

ture determined from x-ray diffraction studies^{22,23} met with little success. The structure puts two molecules, including two H_2O groups and four Li^+ ions in a unit cell with two of the four Li^+ ions surrounded by a tetrahedron of oxygens belonging to sulfate groups. The other two Li ions were supposed to be surrounded by a tetrahedron of oxygens, three of which belonged to sulfate groups, the fourth being the oxygen of the H_2O group. In this manner, since the $\text{Li}-\text{O}$ line, for the H_2O oxygen, was supposed to have two different orientations in the unit cell, but symmetrically disposed with respect to the c -axis, it might be supposed that a large part of the gradient of the electric field responsible for the splitting arises from the field of the strongly polarized water molecule, with one quarter of the lithium ions showing a dependence on the angle measured clockwise from the c -axis, and a second quarter showing the same dependence in terms of the counter clockwise angle. The other half of the Li^+ ions would be relatively little split because of the tetrahedral symmetry of their nearest neighbors. The relative intensities of the satellite lines and the central line would be very small because then, for one orientation, the central line might represent all transitions for $\frac{3}{4}$ of the Li^7 nuclei plus the central line of the remaining $\frac{1}{4}$. Remembering that the squares of the matrix elements giving the line intensities of the $2I$ transitions $m \leftrightarrow m-1$ are proportional to $(I+m)(I-m+1)$, one might expect the area under the satellite line to be only $\frac{1}{10}$ that of the central line. It appears to be about $\frac{1}{5}$, but the very incomplete resolution and the probability that there are different relaxation times, and consequently differing degrees of

²² G. E. Ziegler, *Zeits. f. Krist. Physik* **89**, 459 (1934).

^{21a} The author wishes to thank Dr. G. C. Kennedy for making available this single crystal.

²³ R. W. C. Wyckoff, *The Structure of Crystals* (Rheinhold Publishing Corporation, New York, 1935); *Crystal Structures* (Interscience Publishers, Inc., New York, 1948).

saturation in the two kinds of Li^7 nuclei, makes this aspect of small significance.

The proposed crystal structure would have placed the two protons of a water molecule on a line normal to the c -axis. To check this the splitting, due to the dipole-dipole interaction of the protons, in the proton resonance was observed and found to disagree with such a direction for the proton-proton line. A careful study of this was made by Pake²⁴ in the same sample, who found that there were two distinctly different directions for the proton-proton line, making the angles of $\pm 50^\circ$ with respect to the c -axis. Thus the suggested structure is incorrect in this respect and it seems difficult to fit this new information into the suggested structure for the rest of the elements of the unit cell. The coincidence in the direction of the proton-proton line and that of maximum splitting of the lithium line might suggest a very near proton with resultant splitting of the lithium line by magnetic dipole interaction. This is ruled out because such an interaction would require, to give the observed splitting equivalent to about ± 14 gauss, a $\text{H}-\text{Li}^7$ distance of only about 1.3A. The reciprocal interaction of the Li^7 on the H line would be stronger, because of the large value of μ for Li^7 , and would completely destroy the H-H coupling effect. The incomplete resolution makes further study of this crystal somewhat unrewarding and it has not been investigated further.

The powder pattern of Li_2CO_3 indicates a more hopeful case, because the crystal structure may be simple, being anhydrous, and yet a good splitting is also indicated. Unfortunately, single crystals of this substance have not yet been obtained.

Because of success with NaNO_3 (see below) an

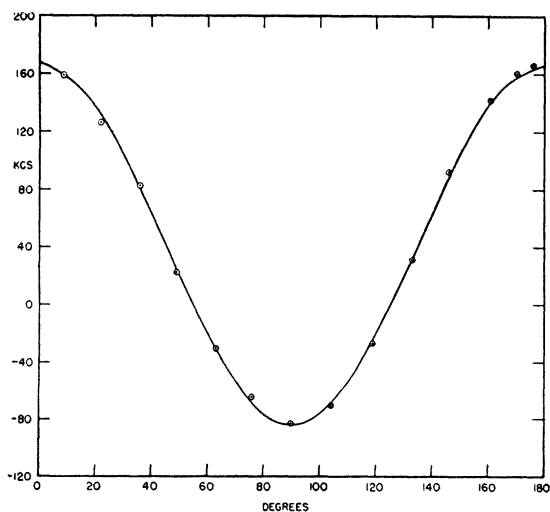


FIG. 6. The frequency interval, in kc, between the central line and the symmetrically placed satellites in NaNO_3 as a function of θ , the angle between H_0 and the crystal axis. The smooth curve is $83.5 (3 \cos^2\theta - 1)$.

²⁴ G. E. Pake, Thesis, Harvard University (1947).

attempt was made to observe the Li^7 resonance in an imperfect and rather small crystal of LiNO_3 , which has the same hexagonal structure as NaNO_3 . The LiNO_3 crystal was grown from aqueous solution at 65°C , to obtain the anhydrous form. The Li^7 resonance was not found and a search for the resonance in a compressed powder pellet, giving a better filling factor than the crystal, revealed only a transient response of one-sided character on the recorder, the sense depending on the direction of approach to resonance. This is interpreted as indicating that the Li^7 relaxation time is very long in this crystal and that it saturates after about two minutes of observation at the level of the oscillator. Therefore the substance could not be used in the pure form for line shape studies. The relaxation effect will be discussed in a later section.

Sodium

The Na^{23} resonance in a single crystal of NaNO_3 shows the anticipated quadrupolar interaction characteristic of an axially symmetric field. The structure²³ is hexagonal with the NO_3^- ions and Na^+ ions lying in planes and with the Na^+ ions on a threefold axis. The crystal was cut with the axis perpendicular to the axis of the cylinder and the spectra obtained for an angle of $0, 54^\circ$ and 90° between the direction of the magnetic

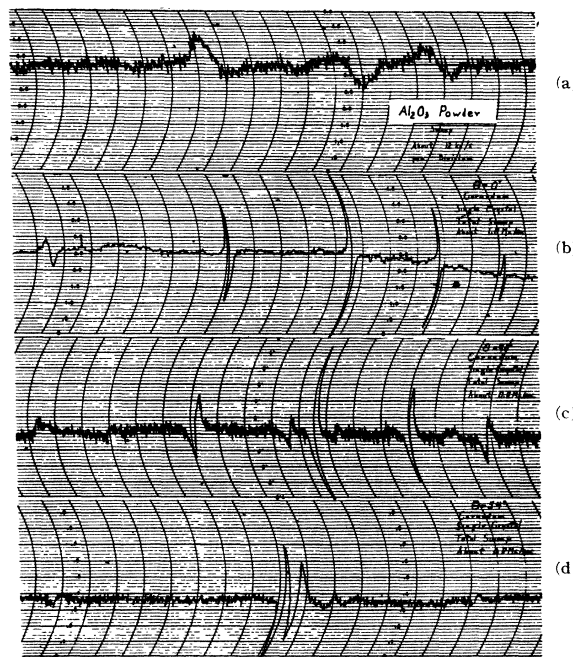


FIG. 7. Spectra of Al^{27} in Al_2O_3 . (a) A powder pattern near 3 Mc with total sweep about 900 kc. (b) A single crystal with hexagonal axis parallel to H_0 . The total sweep is about 1.6 Mc centered at 3 Mc. The 20-sec. time constant is used here. (c) With the crystal axis perpendicular to H_0 , the sweep rate about doubled and the 1-sec. time constant used. (d) With crystal axis at 54° to H_0 , same sweep rate and time constant as in (c).

field and that of the threefold axis of the crystal are reproduced in Fig. 5. The frequency of the central line is about 7.17 Mc and the scale corresponds to about 13 kc per division (equals 15 minutes of time). The 0.05-c.p.s. band width was required to obtain adequate signal-to-noise ratio and several weeks of operating time were required to make about thirty observations of the spectrum at various angles. The breadth of the individual lines is about 2 kc (equivalent to 2 gauss) between points of maximum slope which roughly corresponds to the expected dipole-dipole broadening. The recorded spectrum does not give exactly the derivative of the absorption line since, for sufficient sensitivity, it was found necessary to use a modulation amplitude of the magnetic field of about 2 gauss peak-to-peak, which is not small compared to the line breadth and therefore has an effect on the line shape and width.

For this case the first order perturbation calculation using Eqs. (16) and (18) shows that the satellite lines should fall at frequencies, with spin $\frac{3}{2}$,

$$\nu_{m \rightarrow (m-1)} = \nu_0 + (e^2qQ/4h)(2m-1)[\frac{3}{2} \cos^2\theta - \frac{1}{2}], \quad (20)$$

where ν_0 is the normal pure Zeeman frequency, $\mu H/Ih$. Measurements of the spacings were made only in the $\theta=0$ region, and relative values for other angles were made from the records by averaging the distances between the central line and each of the two satellites. These records were all made in the permanent magnet. The resulting points for 180° of data are plotted on a curve of $83.5(3 \cos^2\theta - 1)$ in Fig. 6 where the fit is seen to be good. The corresponding value of the maximum frequency difference is 167 ± 1 kc, or e^2qQ/h is 334 ± 2 kc. Higher order terms in the perturbation are not required to fit the data within the precision with which the orientation and relative frequencies were measured.

The area under the absorption curves should be in the ratio 3:4:3, in agreement with the ratios of the

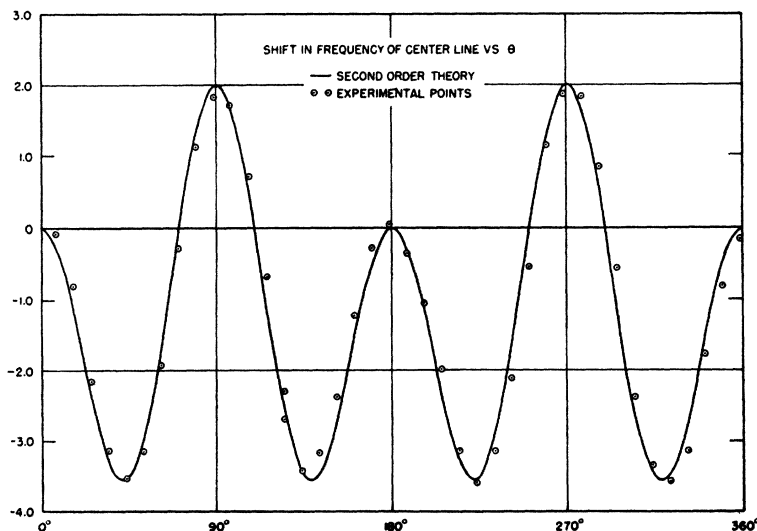
squares of the matrix elements of the three transitions, if the r-f signal were small enough to cause a negligible disturbance in the equilibrium populations of the four levels. The records show a nearly equal response of the spectrograph to all three lines at orientations in which they are definitely separated. Not very much weight should be attached to this result because of the high level of the modulation and the lack of data on the thermal relaxation times. One possible cause may be found, however, in the fact that the line breadths of the three lines may be different, through the operation of term B of Eq. (22) of reference 3 (in which, however, the simultaneous flipping of two spins can only occur adiabatically when the two make the identical transition in opposite senses, with, consequently, a reduction in the contribution of term B compared to the purely magnetic case). A second possibility is the thermal relaxation process if it depends on the electric quadrupole interaction. This will be discussed in a later section.

A comparison of the frequency of the central line, with θ at zero, to that for Na^{23} in a solution of NaBr revealed no difference within the accuracy of measurement of about 200 c.p.s. in 7 Mc.

Aluminum

The record reproduced in Fig. 7(a) resulted with a sample of Al_2O_3 , in the form of a compressed powder, where distinct evidence of a quadrupole splitting is found. The frequency scale was about 900 kc centered near 3 Mc and a field of 2400 gauss was maintained in the small electromagnet. The peculiarly asymmetric and indistinct character of the resonance is best understood in terms of the results with a single crystal.

A natural corundum crystal having distinctly hexagonal external form was cut to form a cylinder with the



† FIG. 8. A plot of the frequency shift of the central line of Al_2O_3 spectrum multiplied by $\nu_0/\Delta\nu^2$, as function of the angle between H and the crystal axis. The solid curve is the theoretical second-order perturbation term, $2(1-9z^2) \cdot (1-z^2)$.

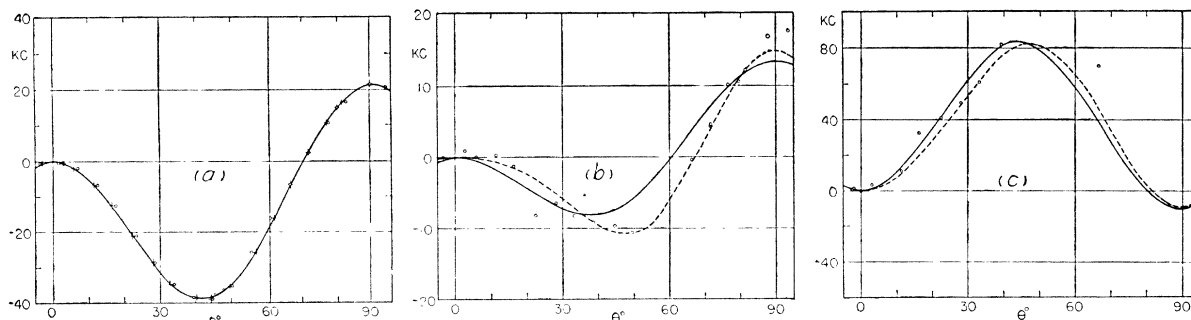


FIG. 9. Higher order perturbation effects in the Al_2O_3 spectrum. (a) The shift in frequency of the central line as a function of the angle θ . The frequency shift is taken as determining the angle from the theoretical second-order curve and this angle is used to evaluate the first-order shifts in the first and second satellite lines. (b) The departure of the first satellite from ν_0 after subtracting $\Delta\nu(3 \cos^2\theta - 1)$. The solid curve is the theoretical second-order term and the broken one is the sum of the second- and third-order terms. (c) The departure of the second satellite line from ν_0 after subtracting $2\Delta\nu(3 \cos^2\theta - 1)$. The value of $\Delta\nu$ is determined independently to be 179.5 kc, from measurements of the spectrum of Fig. 7(b).

axis of the cylinder perpendicular to the hexagonal axis of the crystal. The structure²³ of Al_2O_3 is such that the electric field at the Al^{27} nuclei should be axially symmetric with the same symmetry axis as the crystal. The crystal had a strong coloration, indicative of paramagnetic impurities, and this was expected to give a short spin-lattice relaxation time.^{3,25,26} Figure 7(b) shows the spectrum found with the angle θ , between the magnetic field direction and the crystal axis, at zero. The total sweep here is 1.8 Mc with center again near 3 Mc and the five-line spectrum is confirmation of the spin value of $5/2$. The lines should fall at the frequencies

$$\nu_{m \leftrightarrow (m-1)} = \nu_0 + (3e^2qQ/40h)(2m-1)\left[\frac{3}{2}\cos^2\theta - \frac{1}{2}\right], \quad (21)$$

from first-order perturbation theory, using Eqs. (16) and (18), and where $\nu_0 = \mu H/Ih$. Measurement for $\theta = 0$ showed the frequency spacings to be equal, as accurately as could be determined (± 1 kc), and to be each equal to 359.0 ± 1 kc. Thus the total spectrum covers 1436 kc and is a reasonable fraction of the frequency of the central line.

Figures 7(c) and (d) are records taken for $\theta = 90^\circ$ and for $\theta = 54^\circ$. Here the noise amplitude is greater because the response time of the recorder has been decreased and the sweep rate doubled, to permit a more rapid collection of data. The relaxation time in the crystal was short enough to allow use of a signal level resulting in very adequate response even with the noise pass band in the 1-sec. time constant. In these two records, discrepancies from the first-order perturbation theory show up, the most striking of these being the failure of five lines to converge to a single line at any angle, as they should for the first-order calculation at $(3 \cos^2\theta - 1) = 0$. One can understand this in terms of the effects of the perturbation carried to higher orders where, for instance, one finds that the central line is displaced from the Zeeman frequency ν_0 . The energy differences for the five transitions, carried to terms in the cube of

$e^2qQ/\mu H$ are found to be

$$W\left(\pm\frac{5}{2} \leftrightarrow \pm\frac{3}{2}\right) = h\nu_0 \left\{ 1 \pm 2(3z^2 - 1)\frac{\Delta\nu}{\nu_0} + (33z^2 - 1)(1 - z^2)\left(\frac{\Delta\nu}{\nu_0}\right)^2 \pm \left[60z^2(1 - z^2) - \left(\frac{279z^2 + 6}{4}\right)(3z^2 - 1) \right](1 - z^2)\left(\frac{\Delta\nu}{\nu_0}\right)^3 + \dots \right\}, \quad (22)$$

$$W\left(\pm\frac{3}{2} \leftrightarrow \pm\frac{1}{2}\right) = h\nu_0 \left\{ 1 \pm (3z^2 - 1)\frac{\Delta\nu}{\nu_0} + \left(\frac{5 - 21z^2}{4}\right)(1 - z^2)\left(\frac{\Delta\nu}{\nu_0}\right)^2 \pm \left[\left(\frac{197z^2 - 17}{8}\right) \times (3z^2 - 1) - 60z^2(1 - z^2) \right](1 - z^2)\left(\frac{\Delta\nu}{\nu_0}\right)^3 + \dots \right\}, \quad (23)$$

$$W\left(\frac{1}{2} \leftrightarrow -\frac{1}{2}\right) = h\nu_0 \left\{ 1 + 2(1 - 9z^2)(1 - z^2)\left(\frac{\Delta\nu}{\nu_0}\right)^2 + 0\left(\frac{\Delta\nu}{\nu_0}\right)^4 + \dots \right\}, \quad (24)$$

where $\Delta\nu = 3e^2qQ/40h$, or one-half the frequency interval between lines when $\theta = 0$. Here z is written for $\cos\theta$. The term in these formulas simplest to check experimentally is the term in $(\Delta\nu/\nu_0)^2$ in the central line, $W(\frac{1}{2} \leftrightarrow -\frac{1}{2})$. To measure the frequency at fixed field it was necessary to maintain the magnet current constant by continuous monitoring with a potentiometer across a series resistance. The results are shown in Fig. 8 for a full rotation of the crystal. The circled points represent the data, the shifts in frequency relative to the frequency at $\theta = 0$, multiplied by $(\nu_0/\Delta\nu^2)$, where the $\Delta\nu$ is 179.5 kc as determined above. The smooth curve is the function $2(1 - 9z^2)(1 - z^2)$. Thus there is no arbitrary amplitude

²⁵ R. V. Pound, Phys. Rev. **73**, 523 (1948).

²⁶ N. Bloembergen, Physica **XV**, 386 (1949).

involved in fitting the points to the curve and the agreement is excellent, considering that the maximum frequency difference measured was 37.5 kc with a line breadth of about 4 kc. The main source of experimental error was caused by the somewhat crude mechanism used for rotating the crystal and indicating its position.

To check the theory on the satellite lines, a better indicator was used and frequencies of all lines measured at each of several angles in a 90° interval. The points obtained for the central line are shown in Fig. 9(a). The frequency shift appears to give a better measure of the angle of the crystal than does the mechanical indicator. Therefore the value of θ obtained from assuming the measured frequency to fall on the curve was used to evaluate the term in $\Delta\nu/\nu_0$ in the expressions for the first and second satellite lines. Thus the remaining frequency difference between the satellite line and the central line, at $\theta=0$, after subtracting the values for the term in $\Delta\nu/\nu_0$, is obtained, and plotted in Fig. 9(b) and (c). Here the solid curve is the amplitude of $(\Delta\nu/\nu_0)^2$ and the broken curve is the sum of this and the function in $(\Delta\nu/\nu_0)^3$. The agreement is seen to be as good as could be expected considering the large effect which a small error in angle could introduce through the first-order term. The absence of a third-order, or any

odd-valued order, term in the central-line frequency should be noted.

Several other aspects of this spectrum may be noted. The failure of the lines to converge is in agreement with the second-order effect which would bring, at $(3 \cos^2\theta - 1) = 0$, the central line to $\nu_0[1 - (8/3)(\Delta\nu/\nu_0)^2]$, the first pair of satellites to $\nu_0[1 - \frac{1}{3}(\Delta\nu/\nu_0)^2]$ and the second satellites to $\nu_0[1 + (20/3)(\Delta\nu/\nu_0)^2]$. This is the sense and order of magnitude of the observed effect in Fig. 7(d). In addition to the principal five lines several smaller ones show up, as is evident in Fig. 7(c) and (d). These are explained by the fact that the crystal showed a small amount of striation at an oblique angle, which is believed to correspond to layers of the crystal in a twinned orientation. Thus, in reality, a small part of the sample has a different angle with respect to the magnetic field from that of the main bulk. The records for many angles confirm this explanation.

Something must be said about the relative intensities of the lines. Unfortunately, a constant sensitivity was not obtained with this original spectrograph over such a wide fractional range of frequencies as is covered by this spectrum, but later records taken with the improved spectrograph in the permanent magnet at a 7.2-Mc center frequency indicate that the relative intensities are in the ratio of approximately 25:70:90:70:25. One of these records is reproduced in reference 21. As in the case of Na^{23} , the relative intensities for a sufficiently small signal (avoiding saturation) should be, if the line breadths are equal, that of the squares of the matrix elements, or for spin 5:8:9:8:5. The actual ratio observed is more nearly the square of this and this disagreement is in the opposite sense to that observed for the Na^{23} resonance. The only difference that might be a clue to the opposite sense of the discrepancy seems to be that thermal relaxation in the Al_2O_3 probably results from magnetic interaction with the paramagnetic impurity whereas, in the NaNO_3 , which was optically pure, it probably results through the quadrupole interaction with the lattice. This possibility will be discussed later.

Finally, it may be of interest that the signal-to-noise ratio of the central line of Fig. 7(b) appears to be about what one calculates by methods analogous to those in the appendix of reference 3, assuming the spin system to be unsaturated by the r-f signal of 0.5 volt across the coil. Taking into account the diminution of a single line compared with the unsplit case (see section on the pure quadrupole spectra) and assuming for $T_2 \approx 3 \times 10^{-4}$ sec., one finds a possible amplitude signal-to-noise ratio of about 50 to 1. Thus the noise figure of the spectrograph is not seriously greater than unity.

Iodine

As an example of a nuclear resonance in a single crystal, where the nucleus is known to have a large electric quadrupole moment but where the symmetry

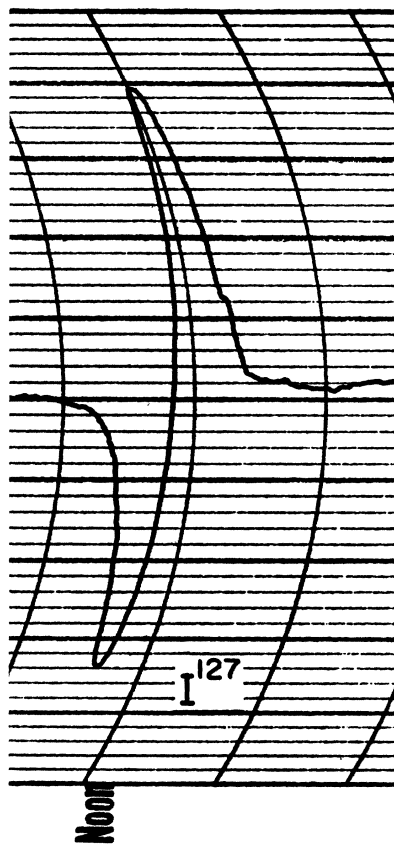


FIG. 10. A record of the line from I^{127} in a single crystal of KI. The frequency is 5.5 Mc and the line is about 600 c.p.s. between the extremes of the derivative.

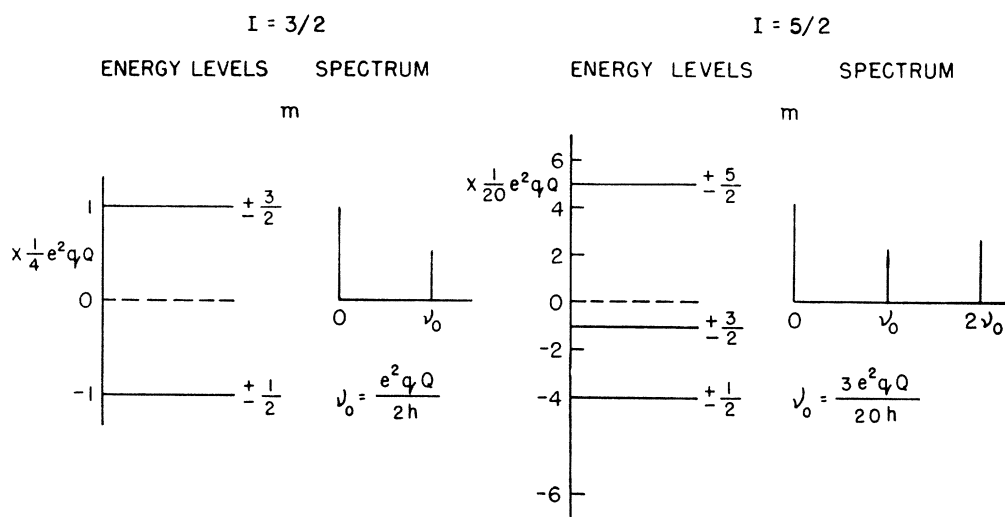


FIG. 11. The energy levels, in zero magnetic field and an axial electric field, for $I=3/2$ and $5/2$, together with the magnetic absorption spectra expected.

of the crystalline field is such that the tensor $\nabla\mathbf{E}$ must be zero, the resonance of I^{127} in a potassium iodide crystal was observed. The line intensity was indicative of the high spin and lack of saturation in the spectrograph indicative of a short relaxation time, although the crystal was probably very free of paramagnetic impurities. In spite of its low g -factor (just $\frac{1}{5}$ that of the proton) an almost noise-free record could be obtained as shown in Fig. 10. This line was found to have a width of only about 600 c.p.s., centered at 5.45 Mc, between points of maximum slope. This is in approximate agreement with the line breadth expected from magnetic dipole-dipole interactions, with the large lattice spacing of the face centered cubic lattice of the I^{127} nuclei. It should be possible, with spin $5/2$, for the nucleus to have an electric sixteen-pole moment, corresponding to the terms with $q=4$ in Eq. (2) and an interaction with the cubic potential would give rise to a splitting. Knowledge of the strength of $\partial^4 V/\partial z^4$ at the position of the nuclei in the crystal would allow an upper limit to be set on the magnitude of the sixteen-pole moment of I^{127} through the evidence that any splitting must be less than about 200 c.p.s.

An attempt was made to produce an electric quadrupole coupling by applying a strong electric field to polarize the crystal. A thin plate-shaped sample was used and an electric field of about 50,000 volts/cm was applied across it, with no detectable change in the line shape or breadth. A perturbation theory calculation leads to an expected effect less than 1 c.p.s., and proportional to the square of the field. Only in ions with very low lying excited levels would such an effect be large enough to be detectable at fields that could be maintained in a crystal.

V. THE PURE ELECTRIC QUADRUPOLE SPECTRUM

One would expect to be able to find nuclear magnetic resonance, through the transition caused by a rotating

magnetic r-f field, without any applied magnetic field, if an electric quadrupole coupling exists. For an axially symmetric potential, the energy levels are then specified by the component of angular momentum, m , taken along the symmetry axis and the levels are given by the formula

$$E_m = \frac{1}{4} [e^2 q Q / I(2I-1)] [3m^2 - I(I+1)]. \quad (25)$$

The resulting energy level schemes for $I=5/2$, and $I=3/2$ are shown in Fig. 11, together with the spectra one would expect to find. For spin $5/2$ the area of the absorption line at higher frequency to that of the lower line for small signal amplitude would be in the ratio 8:5, corresponding to the 4:5 ratio of the squares of the matrix elements, weighted by the factor of 2 ratio of the Boltzman factors $\exp(-h\nu/kT)$. A single crystal would not be needed for detection of this resonance, but, if the line breadth is only that caused by the magnetic dipole interactions, some information about the magnitude of the interaction to be expected in a given crystal would be almost prerequisite to the discovery of the line. The frequencies for the crystals in which the quadrupole coupling has been found are low (718 and 359 kc in Al_2O_3 , for example) and direct observation of these resonances would require special techniques. The available signal-to-noise ratio may be computed by an approach analogous to that in the appendix of reference 3. If a single crystal can be used, with its axis normal to the direction of the oscillating r-f magnetic field, and a small magnetic field along the crystal axis turned on and off, in a square wave fashion, the resonance line may be alternately split into a pair of lines at $\nu_0 \pm (\mu/Ih)H$, where ν_0 is the unperturbed zero-field resonance frequency and h is the paraxial magnetic field. Then a spectrometer such as that used in the experiments described above would record a resonance at ν_0 and two oppositely phased resonances of half the amplitude of the first, one at each side of the main one by the fre-

quency interval $(\mu/Ih)H$. The available signal-to-noise amplitude ratio would be Eq. (62) of reference 3 multiplied by a factor $3(I+m)(I-m+1)/I(I+1)(2I+1)$, if the transitions giving rise to the line are between the states characterized by the paraxial quantum numbers $\pm m$ and $\pm(m-1)$. The factor takes account of the fact that only these levels are involved. Thus the signal-to-noise amplitude ratio expression becomes

$$A_s/A_n = V_c^{\frac{1}{2}} Q_0^{\frac{1}{2}} A \zeta h^2 \gamma N_0 \nu_0^{\frac{1}{2}} T_2^{\frac{1}{2}} (I+m)(I-m+1) / (2I+1) 16kT(kTBF)^{\frac{1}{2}} T_1^{\frac{1}{2}}, \quad (26)$$

where all symbols have the same significance as in reference 3. It should also be observed that this same expression, divided by 2, gives the available signal-to-noise ratio for the individual component lines in a strong magnetic field. Thus the line at 719 kc in Al_2O_3 in zero field should have a signal-to-noise ratio for the same sample only about 1/20 as great as that of the central line in the spectrum of Fig. 7(b).

Advantage can be taken, however, of the absence of the magnetic field in that there is then no restriction, from field inhomogeneity requirements, on the size of the sample, and thus on V_c . The gain available here can only be utilized, however, if a spectrometer of as small a noise figure can be made to operate at a correspondingly higher r-f power level, so that the same energy density is obtained in the sample volume.

If a powder is used instead of a single crystal, the same modulation scheme would work except that the line would be smeared out in the half-period that the modulation field was on because of the random orientation of microcrystals with respect to the field. The absorption at ν_0 in the half-period when the modulated field is absent would be smaller than that for a properly oriented crystal by a factor $\frac{2}{3}$ resulting from averaging the square of the component of the r-f magnetic field in the plane normal to a crystal axis over the uniform distribution of orientations of the crystals.

A much higher frequency, and correspondingly stronger resonance, resulting from the electric quadrupole splitting, would be expected in certain molecular crystals composed of molecules such as ICl, CH_3I , and others, where values of e^2qQ are known for the gaseous state from microwave spectroscopy. In ICl, for example, the iodine interaction²⁷ is 2930 Mc and lines near 879 and 439 Mc would be expected.

An unsuccessful attempt to detect the pure electric quadrupole spectrum of I^{127} in ICl has been made with a c-w oscillator fed into a capacitatively loaded coaxial-line resonator, with tuning provided by variation of the capacity. In this way, a frequency range from about 600 to 1200 Mc was covered. The cavity had a loaded Q of about 600 when operated as a transmission filter feeding a crystal detector. The ICl was contained in a glass doughnut-shaped liner filling the inductive part of the cavity. The r-f oscillator was frequency modulated at

60 c.p.s. by a rotating wire inserted into the oscillator cavity and a swing of about 100 kc peak-to-peak was obtained. The crystal detector output was observed on an oscilloscope synchronized at 60 c.p.s. and r.m.s. noise voltage was less than about 0.1 percent of the detected voltage. Thus resonances sharper than the f-m swing should have been found as a bump in the trace as the system was scanned manually in frequency.

That such a resonance was not found indicated that at the lowest temperature used (90°K) the resonance was either outside the search range or too broad to have sufficient intensity to result in a 0.1 percent absorption. If the latter were assumed to be the cause, an approximate lower limit on the breadth may be set, since the fractional power absorption should be $\Delta P/P_0 = 2Q_L\delta$, where δ is the reciprocal Q of the resonance. The quantity δ is given by Eq. (56) of reference 3, multiplied by $3(I+m)(I-m+1)/I(I+1)(2I+1)$, with $I=m=5/2$, as discussed above, and multiplied by $\frac{2}{3}$ because the sample is a polycrystalline material. Another factor of $\frac{1}{2}$ may be included as an estimate of the filling factor for the sample in the cavity. In this manner, a line breadth of greater than about 100 kc may be estimated to be compatible with the resonance being present in the interval of frequency covered but being undetected.

A possible explanation for the failure to find a resonance in the range is that the line is broader than 100 kc. The broadening to be expected from magnetic dipole interactions is only of the order of magnitude of 1 kc but there exists the possibility that the presence of thermally excited states of torsional oscillation of the diatomic molecules²⁸ would produce, through the then time dependent electric quadrupole interaction, a very strong relaxation mechanism, with consequent broadening. Such excited states would not necessarily be frozen out at the temperature of liquid nitrogen. A similar broadening would be expected if the diatomic molecules made end for end flips in times less than say 10^{-4} sec. Evidence of such transitions can be obtained from observation of the dielectric dispersion because the ICl molecule has an electric dipole moment.

Evidence of the existence of this dispersion was obtained by placing the doughnut in the center of a short-circuited coaxial line resonator of about seven inches length. From the decrease in Q and the change in the resonant frequency with and without the doughnut containing the ICl, a rough estimate could be made of both the real and imaginary parts of the dielectric constant of the ICl at various temperatures. Because of the presence of the glass container and uncertainty about the density of the ICl in it, the experiment served only to show orders of magnitude. The real part of the dielectric constant appeared to be about 6, and did not change appreciably with temperature. Strong electric absorption was found at 0°C and, as expected, it

²⁷ Townes, Wright, and Merritt, Phys. Rev. **73**, 1334 (1948).

²⁸ L. Pauling, Phys. Rev. **36**, 430 (1930).

decreased rapidly with temperature, becoming indistinguishable from the losses of the resonator itself at -75°C . If the frequency of end-over-end flipping of the molecules is assumed to follow a law of the form $\nu = \nu_0 \exp(E/kT)$, one is led to conclude that this cause of broadening should not be severe at liquid nitrogen temperatures.

Recently Dehmelt and Krueger²⁹ have found the two absorption lines caused by the electric quadrupole splitting for the chlorine isotopes Cl^{35} and Cl^{37} in *trans*_{1,2}-dichloroethylene in the region of 35 Mc. They found the lines to be about 10 kc in breadth at 90°K and to broaden as the temperature was raised.^{29a} If this breadth is caused by an electric quadrupolar relaxation mechanism, the effect might be about 1000 times larger in the I^{127} resonance in ICl , because of the 30 times larger electric quadrupole coupling. Therefore, the experiment with ICl is about to be tried at liquid helium temperatures. If the existence of such a large electric quadrupole coupling in the crystalline state can be proven, it may be useful for the alignment of nuclei in space at very low temperatures.³⁰ The fact that the chlorine resonances are near to the frequencies one would expect from the coupling observed in molecules³¹ like CH_3Cl is evidence in support of the existence of the larger couplings for nuclei of large electric quadrupole moment.

With a single crystal one would expect to be able to demonstrate the existence of a large electric quadrupole interaction by observation of the resonance in a magnetic field at the normal frequency determined by the *g*-factor of the nucleus for an odd half-integral spin. The levels $m = \pm \frac{1}{2}$ are degenerate in the absence of a magnetic field with an electric field of axial symmetry. With a magnetic field applied along the symmetry axis, the Hamiltonian is diagonal and the energy difference between the levels $m = \pm \frac{1}{2}$ is simply $\mu H_0/I$ for all relative magnitudes of μH and e^2qQ . If the crystal were rotated, however, so that the field and the axis make an angle θ with respect to one another, one has a much more difficult problem. It is clear that the resulting frequency shift must depend on the relative magnitudes of e^2qQ and μH .

For an axial field and a spin of $\frac{3}{2}$, the problem can be solved in closed form for $\theta = 90^{\circ}$. The non-vanishing matrix elements of the combined electric quadrupole and magnetic interaction, in a scheme with the *z* direction as the crystal axis are

$$\begin{aligned} (\pm \frac{3}{2} | \mathcal{H} | \pm \frac{3}{2}) &= -a \pm \frac{3}{2} b \cos \theta, \\ (\pm \frac{1}{2} | \mathcal{H} | \pm \frac{1}{2}) &= a \pm \frac{1}{2} b \cos \theta, \\ (\pm \frac{3}{2} | \mathcal{H} | \pm \frac{1}{2}) &= (\pm \frac{1}{2} | \mathcal{H} | \pm \frac{3}{2}) = \frac{1}{2} 3^{\frac{1}{2}} b \sin \theta, \\ (\pm \frac{1}{2} | \mathcal{H} | \mp \frac{1}{2}) &= b \sin \theta, \end{aligned} \quad (27)$$

where

$$a = e^2qQ/4, \quad b = \mu H/I.$$

The resulting quartic secular equation has been solved³² for $\theta = 90^{\circ}$ and the energies of the middle two of the four levels become

$$E_{\pm \frac{1}{2}} = \pm \frac{b}{2} - (b^2 \mp ab + a^2)^{\frac{1}{2}}. \quad (28)$$

Since we are interested in the case $a \gg b$, the radical may be expanded by the binomial theorem and one finds for the energy difference

$$\Delta W_{\frac{1}{2} \leftrightarrow -\frac{1}{2}} \approx 2b \left[1 - \frac{3}{16} \left(\frac{b}{a} \right)^2 + \dots \right]. \quad (29)$$

Note that for $a \rightarrow \infty$, the line moves to just twice its normal frequency, which is a result previously noted by Ramsey.³³ For a finite value of e^2qQ , the frequency will not be quite doubled. If one denotes by ν_m the frequency for $\theta = 0$, $R\nu_m$ the frequency for $\theta = 90^{\circ}$ where $1 \leq R < 2$, and ν_e the electric quadrupole splitting in zero magnetic field, one finds

$$\nu_e = \left(\frac{3}{2} \right)^{\frac{1}{2}} \nu_m / (2 - R). \quad (30)$$

For transitions to be induced by the r-f signal field, it is apparent that the crystal axis should be made normal to both the applied static magnetic field and the r-f magnetic field. A similar effect should result for higher odd-valued half-integral spins but the secular equations may have to be solved by numerical methods. Detection of this resonance would probably also require low temperatures to reduce broadening by thermally excited motions of the molecules.

VI. RELAXATION EFFECTS

It is well recognized that the coupling between the nuclear spin system and lattice vibrations, in a rigid crystal lattice, through the magnetic dipolar interactions of the nuclei, fails to account for the relaxation times commonly found in crystals at room temperature. Instead, most solids in which relaxation times have been studied have been found to contain either some kind of paramagnetic impurity which greatly shortens the relaxation time,²⁶ or a rotating or jumping constituent nucleus or complex group, also resulting in shortened relaxation time.³⁴⁻³⁶

Several of the crystals used in the experiments described above were probably of very high purity, notably the NaNO_3 and the KI crystals, both of which were obtained from the Harshaw Chemical Company. Although relaxation times were not measured, the strength of the iodine resonance in KI was such as to

²⁹ Dehmelt and Krueger, *Naturwiss.* [to be published; reported in the *European Scientific Notes of ONR*, London, 3, 379 (1949)].

^{29a} The author wishes to thank Professor H. Kopferman for communicating some details of these results prior to publication.

³⁰ R. V. Pound, *Phys. Rev.* 76, 1410 (1949).

³¹ Gordy, Simmons, and Smith, *Phys. Rev.* 72, 344 (1947).

³² Whitmer, Weidner, Hsiang, and Weiss, *Phys. Rev.* 74, 1478 (1948).

³³ N. F. Ramsey, *Phys. Rev.* 74, 286 (1948).

³⁴ A. M. Sachs, Thesis, Harvard University (1950).

³⁵ E. H. Turner, Thesis, Harvard University (1950).

³⁶ R. Newman, *J. Chem. Phys.* (to be published).

indicate negligible saturation at the level of the spectrograph, whereas the sodium lines in NaNO_3 indicated partial saturation. This would indicate that the relaxation time of I^{127} in KI was less than about 0.02 sec. and that of Na^{23} in NaNO_3 less than about 0.5 sec. On the other hand, a relaxation time of about two hours was indicated in the Li^7 resonance in LiNO_3 from a study of the transient response, previously described, as a function of the time the system was allowed to stand in the magnetic field between observations of the resonance. Although the electric quadrupole moment of Na^{23} is not known, it is probably larger than that of Li^7 and smaller than that of I^{127} . This is substantiated by the fact that no evidence of a large splitting was observed in the transient LiNO_3 resonance in contrast with the triple Na^{23} resonance in the isomorphous NaNO_3 crystal. Thus one is led to suggest that the thermal relaxation can result from the electric quadrupolar interaction.

Consider a situation in which any quadrupolar splitting of the nuclear resonance in a magnetic field is small compared to the magnetic resonance frequency itself. In Eqs. (16) we see that the electric quadrupole interaction operator has elements corresponding to changes of m by ± 1 and ± 2 , as well as the diagonal elements. Vibrations of the lattice result in time dependence of the quantities $(\nabla E)_{\pm 1}$ and $(\nabla E)_{\pm 2}$ and, in analogy to the magnetic dipole interaction discussed in reference 3, one can make a Fourier transformation of these time dependent quantities into their equivalent spectral densities as functions of frequency. In this manner, one finds that the energy in the region of $\pm \nu_0$, where ν_0 is the nuclear resonance frequency in the strong magnetic field, causes non-adiabatic transitions corresponding to $\Delta m = \pm 1$ and that of $(\nabla E)_{\pm 2}$ at $\pm 2\nu_0$ causes transitions corresponding to $\Delta m = \pm 2$. Because a thermal mechanism is involved, downward transitions are weighted more heavily than upward ones by the Boltzmann factor $\exp(h\nu_0/kT)$ and $\exp(2h\nu_0/kT)$ for the changes in $|m|$ of 1 and 2 respectively. Even though there may be no static electric quadrupole interaction, and so no splitting observed, in a field of cubic symmetry in the time average, the field departs from this symmetry during the periods of the lattice vibrations, and a relaxation mechanism is provided. To compute the relaxation times expected, the magnitudes and spectral densities of the functions $(\nabla E)_{\pm 1}$ and $(\nabla E)_{\pm 2}$ must be known. Involved in them are the knowledge of the amplitudes of the lattice vibrations and the shielding effect of the electrons surrounding the nucleus. These will not be dealt with here. Most of the vibrational frequencies are large compared to ν_0 . As in the case of the magnetic interaction, because both involve the time dependence of the same functions of θ , ϕ , and r^{-3} , it will be true that a "second-order" effect involving absorption at ν and re-emission at $\nu - \nu_0$ or $\nu - 2\nu_0$, which can operate over the full range of the spectral densities will be the dominant effect.⁴

The relaxation time from this interaction may be estimated by comparison with magnetic case by noting that in its vibration a nucleus varies its distance to a nearby charged ion in the same way as it varies its distance to a nearby nuclear magnetic dipole. Therefore, the magnetic and electric interaction energies for such a pair will be e^2Q/r^3 and μ^2/r^3 respectively. The ratio is simply e^2Q/μ^2 and the ratio of the resulting relaxation times is approximately the square of the interaction energy ratio, $(e^2Q)^2/\mu^4$. For a moderately large value of Q of 10^{-25} cm² and a μ of 10^{-23} gauss cm³, we find the ratio is 6.25×10^4 , or the electric quadrupole interaction leads to relaxation times of the order of fractions of seconds if the magnetic one leads to relaxation times of several hours. Because all charged neighbors, and possibly to some extent the electron system of the nucleus itself, can contribute to the quadrupole interaction, instead of only those neighbors having magnetic moments, the ratio should be even larger. Of course, the effects of motions of molecules in molecular crystals considered in the last section might be much larger yet because of the very much larger values of the quadrupole interaction energy.

As further evidence that such an effect is present, consider the spectrum of the cubic alkali-halide crystal NaBr. There are three resonances in a narrow (about 10 percent) region of frequency corresponding to the Na^{23} and the two equally abundant (50 percent each) isotopes Br^{79} and Br^{81} . All three of these nuclei have spins of $\frac{3}{2}$ and electric quadrupole moments. Because of the small differences in their magnetic moments, any relaxation process depending on magnetic interaction should result in nearly equal relaxation times. Such is not the case, as may be seen from Fig. 12, in which the resonances of Na^{23} and Br^{81} are shown at each of three levels of the spectrometer. At 0.12 volt r.m.s. across the coil, the Na^{23} is about double the intensity of the Br resonance, as it should be at a signal level low enough to result in negligible saturation, because this is the abundance ratio. At 0.5 volt r.m.s., however, the Na^{23} line is reduced relatively to the Br^{81} line so that they are nearly equal in amplitude and finally at 1 volt, the Br^{81} line is about twice as intense as the Na^{23} line. Thus an electric quadrupolar relaxation mechanism is indicated and the Na^{23} electric quadrupole interaction is seen to be smaller than that of Br^{81} . It is possible that careful measurement of relative magnitudes of relaxation times of several nuclei in crystals as simple as this could yield valuable information on the relative magnitudes of electric quadrupole moments. Care must be taken to eliminate paramagnetic impurities. This has not been done with the NaBr sample.

The very long relaxation time observed in LiNO_3 must be the result of two special situations. First, the smallness of the electric quadrupole moment of Li^7 makes the relaxation from the quadrupole coupling long. Many crystals, such as CaF_2 and LiCl have, however, shorter relaxation times. The F^{19} resonance in

CaF₂ can only be relaxed by magnetic interactions since the spin is $\frac{1}{2}$, and Bloembergen has shown²⁶ strong correlation between the presence of paramagnetic impurities and the relaxation times in various samples of CaF₂. In crystals such as LiCl, however, there may be present chemically undetectable paramagnetic impurities in the form of F centers, which one might expect to be much less easily produced in LiNO₃ and this may be the explanation for the considerably shorter relaxation times commonly observed in LiCl. An investigation of this possibility is being undertaken.

An electric quadrupolar relaxation mechanism seems able to account for the nearly equal intensities of the three Na²³ lines in NaNO₃. This may be understood if one considers the differential equations for the time dependence of the populations of the four levels, for spin $\frac{3}{2}$, in the presence of both a magnetic r-f signal and either a magnetic or electric quadrupolar energy spectrum derived from thermal sources bringing about thermal relaxation.

First consider the case of a magnetic relaxation process. Both the applied signal and the thermal process have matrix elements corresponding to $\Delta m = \pm 1$ and we can write for a signal applied at the $\frac{3}{2} \leftrightarrow \frac{1}{2}$ satellite frequency,

$$\begin{aligned} \dot{N}_{\frac{3}{2}} &= -(W_{\frac{3}{2} \rightarrow \frac{1}{2}} + p_{\frac{3}{2} \rightarrow \frac{1}{2}})N_{\frac{3}{2}} + (W_{\frac{1}{2} \rightarrow \frac{3}{2}} + p_{\frac{1}{2} \rightarrow \frac{3}{2}})N_{\frac{1}{2}}, \\ \dot{N}_{\frac{1}{2}} &= (W_{\frac{3}{2} \rightarrow \frac{1}{2}} + p_{\frac{3}{2} \rightarrow \frac{1}{2}})N_{\frac{3}{2}} - (W_{\frac{1}{2} \rightarrow \frac{3}{2}} + W_{\frac{1}{2} \rightarrow -\frac{1}{2}} + p_{\frac{1}{2} \rightarrow \frac{3}{2}})N_{\frac{1}{2}} \\ &\quad + W_{-\frac{1}{2} \rightarrow \frac{1}{2}}N_{-\frac{1}{2}}, \\ \dot{N}_{-\frac{1}{2}} &= W_{\frac{3}{2} \rightarrow -\frac{1}{2}}N_{\frac{3}{2}} + W_{-\frac{1}{2} \rightarrow -\frac{3}{2}}N_{-\frac{3}{2}} \\ &\quad - (W_{-\frac{1}{2} \rightarrow \frac{1}{2}} + W_{-\frac{1}{2} \rightarrow -\frac{1}{2}})N_{-\frac{1}{2}}, \\ \dot{N}_{-\frac{3}{2}} &= W_{-\frac{1}{2} \rightarrow -\frac{3}{2}}N_{-\frac{1}{2}} - W_{-\frac{3}{2} \rightarrow -\frac{1}{2}}N_{-\frac{3}{2}}, \end{aligned} \quad (31)$$

where the W 's arise from thermal processes and the p 's from the applied signal. These relations can be simplified with the following relationship

$$\begin{aligned} W_{-\frac{3}{2} \rightarrow -\frac{1}{2}} &= W_{\frac{1}{2} \rightarrow \frac{3}{2}} = 3W, \\ W_{-\frac{1}{2} \rightarrow -\frac{3}{2}} &= W_{\frac{3}{2} \rightarrow \frac{1}{2}} = 3W \exp(h\nu_0/kT) \approx (1+\Delta)3W, \end{aligned}$$

where $\Delta = h\nu_0/kT$,

$$\begin{aligned} W_{-\frac{1}{2} \rightarrow \frac{1}{2}} &= 4W, \quad W_{\frac{1}{2} \rightarrow -\frac{1}{2}} \approx (1+\Delta)4W, \\ p_{\frac{3}{2} \rightarrow \frac{1}{2}} &= p_{\frac{1}{2} \rightarrow \frac{3}{2}} = 3p, \end{aligned} \quad (32)$$

where $p = \frac{1}{4}\gamma^2 H_1^2 g(\nu)$, and γ , H_1 and $g(\nu)$ have the same significance as in Eq. (4) of reference 3. In this manner one obtains

$$\begin{aligned} \dot{N}_{\frac{3}{2}} &= W \{-3(1+\Delta+P)N_{\frac{3}{2}} + 3(1+P)N_{\frac{1}{2}}\}, \\ \dot{N}_{\frac{1}{2}} &= W \{3(1+\Delta+P)N_{\frac{3}{2}} - (7+4\Delta+3P)N_{\frac{1}{2}} + 4N_{-\frac{1}{2}}\}, \\ \dot{N}_{-\frac{1}{2}} &= W \{4(1+\Delta)N_{\frac{3}{2}} - (7+3\Delta)N_{-\frac{1}{2}} + 3N_{-\frac{3}{2}}\}, \\ \dot{N}_{-\frac{3}{2}} &= W \{3(1+\Delta)N_{-\frac{1}{2}} - 3N_{-\frac{3}{2}}\}, \end{aligned} \quad (33)$$

where $P = p/W$. Assuming a steady state to be maintained as the line is swept through slowly, all terms on the left side may be taken to be zero and one obtains

$$\begin{aligned} N_{-\frac{3}{2}} &= (1+\Delta)N_{-\frac{1}{2}}, \quad N_{-\frac{1}{2}} = (1+\Delta)N_{\frac{1}{2}}, \\ N_{\frac{3}{2}} &= [1+\Delta/(1+P)]N_{\frac{1}{2}}. \end{aligned} \quad (34)$$

With the restriction that $N_{\frac{3}{2}} + N_{\frac{1}{2}} + N_{-\frac{1}{2}} + N_{-\frac{3}{2}} = N$, the

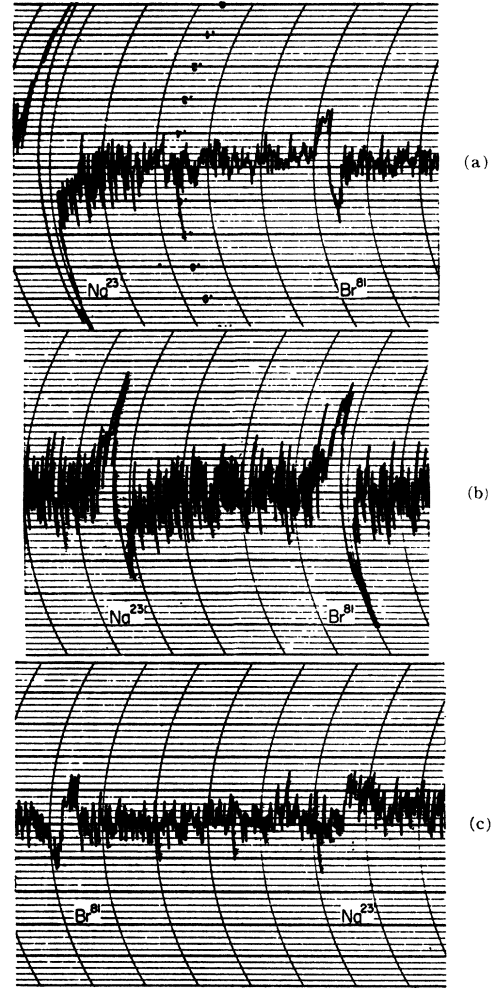


FIG. 12. The Na²³ and Br⁸¹ resonances in NaBr show different relaxation times. In (a) and r-f signal level of 0.12 volt is used, in (b) about 0.5 volt, and in (c) about 1 volt across the r-f coil. The tuning capacity was about 150 μmf and with the coil volume of about 5 cc the resulting magnitudes of the rotating magnetic field H_1 are 0.005, 0.02, and 0.04 gauss, respectively.

total number of the subject nuclei in the sample, we find that the effect of a signal at the line corresponding to the $\frac{3}{2} \rightarrow \frac{1}{2}$ transition alters the zero signal population differences only in a second order in Δ for the other two lines but that

$$N_{\frac{3}{2}} - N_{\frac{1}{2}} \approx -\frac{N}{4} [1/(1+P)] (h\nu/kT) = n_0 [1/(1+P)], \quad (35)$$

where n_0 is the equilibrium, zero signal, population difference for all three possible transitions.

A repetition of the above calculation with the signal placed for absorption by the $\frac{1}{2} \rightarrow -\frac{1}{2}$ transition gives the same result for the saturation factor of the central line,

$$N_{\frac{3}{2}} - N_{-\frac{1}{2}} \approx n_0 [1/(1+P)], \quad (36)$$

as a result of the fact that $p_{\frac{1}{2} \leftrightarrow -\frac{1}{2}} = 4p$ for this case, assuming the three line shape factors to be identical. The conclusion then is that even for a signal so large that P is not negligible compared to unity, so long as the r-f field strength is held constant, the three lines should be in the same relative amplitudes to one another as at very low signal levels. Furthermore, if a large signal is applied at one transition frequency, the absorption of a small signal at the other two lines would be unaffected so long as $h\nu \ll kT$. A similar argument must hold for other spin values.

By contrast, consider the situation if an electric quadrupole interaction causes the relaxation. The second and third parts of Eq. (16) may be considered as time dependent because of the thermal vibrations of the crystal which cause the quantities $(\nabla E)_{\pm 1}$ and $(\nabla E)_{\pm 2}$ to be time dependent. Non-adiabatic transitions of the spin system can then be produced and transitions downward with $\Delta m = 1$ and $\Delta m = 2$ must be more heavily weighted than those upward by the factors $\exp(h\nu_0/kT)$ and $\exp(2h\nu_0/kT)$ respectively. Assuming the "second-order" mechanism to be dominant, each frequency in the vibrational spectrum will contribute to both $\Delta m = 1$ and to $\Delta m = 2$ and one must integrate over the whole spectrum of the crystalline vibrations. In this way, one finds the only non-vanishing upward transition probabilities to be

$$W_{-\frac{1}{2} \rightarrow \frac{1}{2}} = W_{-\frac{3}{2} \rightarrow \frac{1}{2}} = W_{\frac{1}{2} \rightarrow \frac{3}{2}} = W_{-\frac{3}{2} \rightarrow \frac{3}{2}} = W_e \quad (37)$$

from Eqs. (16) and (18). This result is calculated from the fact that the transition probability $W_{m \rightarrow m'} \propto |m|F|m'|^2$. Accordingly, the downward transition probabilities are

$$\begin{aligned} W_{\frac{1}{2} \rightarrow -\frac{1}{2}} &= W_{-\frac{1}{2} \rightarrow -\frac{1}{2}} \approx (1 + \Delta)W_e, \\ W_{\frac{3}{2} \rightarrow -\frac{1}{2}} &= W_{\frac{3}{2} \rightarrow -\frac{3}{2}} \approx (1 + 2\Delta)W_e. \end{aligned} \quad (38)$$

An analysis can be carried out, in a manner analogous to that given above for the magnetic case, to find the steady state populations of the levels in the presence of an applied signal at the frequency of the $\frac{3}{2} \leftrightarrow \frac{1}{2}$ transition, and again at the $\frac{1}{2} \leftrightarrow -\frac{1}{2}$ transition. For the signal applied at the $\frac{3}{2} \leftrightarrow \frac{1}{2}$ transition the results are

$$\begin{aligned} N_{\frac{1}{2}} - N_{\frac{3}{2}} &\approx [1 - 3P_e/(4 + 9P_e)][2/(2 + 3P_e)]n_0, \\ N_{-\frac{1}{2}} - N_{\frac{1}{2}} &\approx [(4 + 15P_e)/(4 + 9P_e)]n_0, \\ N_{-\frac{3}{2}} - N_{-\frac{1}{2}} &\approx [1 - 3P_e/(4 + 9P_e)]n_0, \end{aligned} \quad (39)$$

where $P_e = p/W_e$. For the signal applied at the $\frac{1}{2} \leftrightarrow -\frac{1}{2}$ transition, the central line, the steady state populations yield

$$\begin{aligned} N_{\frac{1}{2}} - N_{\frac{3}{2}} &= [1 + 2P_e/(1 + 4P_e)]n_0, \\ N_{-\frac{1}{2}} - N_{\frac{1}{2}} &= [1/(1 + 4P_e)]n_0, \\ N_{-\frac{3}{2}} - N_{-\frac{1}{2}} &= [1 + 2P_e/(1 + 4P_e)]n_0. \end{aligned} \quad (40)$$

Comparison of $N_{\frac{1}{2}} - N_{\frac{3}{2}}$ of Eqs. (39) with $N_{-\frac{1}{2}} - N_{\frac{1}{2}}$ of Eqs. (40) shows that at a given level of signal power, corresponding to a given value of P_e , the satellite line is relatively less saturated than is the central line, and this has the effect of increasing the apparent intensities

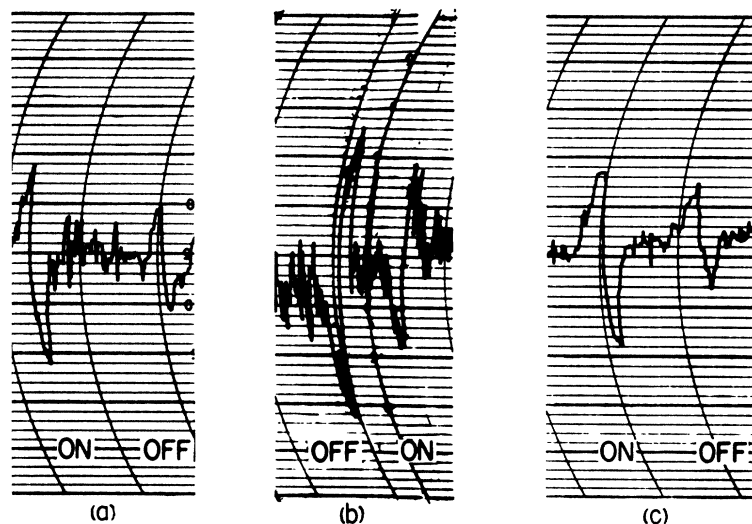
of the satellite lines relative to that of the central one. Therefore, instead of the 3:4:3 amplitude ratio expected at negligible saturation, the amplitude ratios of the peak absorption itself become 4:3:4 in the limiting case of $P_e \gg 1$. The recorded lines are, of course, not the absorption but a signal derived from it through the modulation of the magnetic field and, for a modulation amplitude approaching the line width, the recorded amplitudes should behave in a manner similar to that of the lines themselves.

Thus the electric quadrupolar relaxation is able to account for the near equality of the three lines in the Na^{23} spectrum in NaNO_3 . Optimum signal-to-noise ratio results for P_e near unity and, unfortunately, the recorded line strength was not large enough to allow a good test of this theory to be made by observations at lower and higher power levels, because the signal-to-noise ratio became poorer for levels differing in either direction. An interesting test of the theory appears possible by the observation of one line with a low applied signal level while simultaneously heavily saturating another. Thus in Eqs. (39) one sees that saturation of a satellite line should raise the small-signal intensity of the central line to 5/3 its normal intensity. No effect of this kind is present in the purely magnetic case, as is evident from Eqs. (35).

Such an experiment has been carried out. The cylindrical NaNO_3 crystal was so filed as to have two parallel flat faces perpendicular to the axis of the crystal and a coil was wound lengthwise around it. Thus, when the crystal was inserted into the r-f coil of the spectrograph, with its axis along the magnetic-field direction, the axis of the new coil was perpendicular to both the magnetic-field direction and the axis of the spectrograph coil. The new coil was resonated with a series condenser of about 15 μmf . This series resonant circuit could be driven with an r-f current in the range of the Na^{23} spectrum from a GR 805-C signal generator. The orthogonality of the two r-f coils was required to minimize their interaction.

The frequency of the auxiliary signal generator was first set exactly at the frequency of the upper satellite line. A record of the central line was made with the spectrograph at a low level (about 0.5 volt r.m.s. across the coil) with the auxiliary signal generator off. The record was then repeated with the auxiliary signal generator supplying 0.2 volt r.m.s. across the series resonant circuit and the central line was found to be approximately doubled in amplitude. On the other hand, when the same experiment was repeated, but at the frequency of the lower satellite line, with the saturating signal still applied at the upper line, the intensity observed with the saturation signal on was only about $\frac{2}{3}$ that found with it off. Finally, the saturation signal was moved over to the frequency of the central line and the effect on the lower satellite observed. This time, to avoid a change in sensitivity of the spectrograph between the two runs from the interaction with the strong applied signal, the auxiliary generator

FIG. 13. (a) Record of change in intensity of the central line in the NaNO_3 spectrum of Fig. 5 from simultaneously saturating the upper satellite line. The central line with the saturation signal on is about double its normal intensity. (b) The lower satellite line, which is only $2/3$ its normal intensity when the saturation signal at the upper satellite is applied. (c) A satellite line is increased to $3/2$ times its normal intensity by the application of the saturation signal at the central line.



was kept at a constant level but shifted about 14 kc to be away from the central line on one run. The observed line amplitude with the saturation signal applied was almost exactly $\frac{3}{2}$ times the normal level, in agreement with Eq. (40) for $P_e > 1$. The records obtained in these experiments are reproduced in Fig. 13(a), (b), and (c). The agreement of these results with the predictions of Eqs. (39) and (40) must be considered very strong evidence that the thermal equilibrium of the spin system with the lattice is brought about by the electric quadrupole interaction.

VII. CONCLUSIONS

It is seen that the possession of an electric quadrupole moment by a nucleus can strongly affect the nuclear resonance spectrum found. For such nuclei in solids of lower than cubic symmetry a nuclear resonance signal may be expected to be observable in a polycrystalline sample only if the electric quadrupole moment is very small, such as that of Li^7 , or in the absence of a static magnetic field. Otherwise the resonance lines are smeared out, as in the Al_2O_3 powder, because of the distribution of directions of crystal axes, and the absorption is very weak. To observe resonances in single crystals, the crystals must be of relatively simple structure to avoid the splitting up of the total absorption into a large number of weak lines. Very large splittings may be expected. This is especially true for molecular crystals in which the splittings may be very large compared to the magnetic energy differences obtainable. It is probable in these cases that relaxation mechanism provided by the thermal oscillations of the molecules about their rest positions are so strong as to greatly broaden the resonance lines and render them detectable only at very low temperatures.

Strong evidence is found for supposing that the principal relaxation mechanism, for nuclei of spin

greater than $\frac{1}{2}$, is the electric quadrupole coupling, in ionic as well as molecular crystals of all symmetries, unless considerable paramagnetic impurity is present, as it was in the Al_2O_3 crystal.

Unfortunately, no information concerning the sign of the quadrupole coupling energy is obtained from either the pure electric quadrupole spectrum or that of the combined magnetic and electric interactions, unless temperatures such that $h\nu/kT \sim 1$ could be reached. This is in the realm of possibility with such large electric quadrupole interactions as that of I^{127} in ICl , for instance.

As in other cases of observation of electric quadrupole interactions, only a quantity dependent on both the quadrupole moment and its surroundings is determined from these spectra. In the case of fields of axial symmetry the measured quantities can be designated as e^2qQ . The magnitude of Q can be determined only if q can be determined independently. In this connection, ionic crystals, such as the NaNO_3 (but preferably simpler ones), may prove useful. Here the ion of the nucleus in question is very often in a singlet- S state and would not be expected to contribute independently to q . The other ions in the crystal, especially if they are monatomic ions, may be treated as point charges and a value of q determined from the relation

$$eq = \sum_j (3 \cos^2\theta - 1) r_j^{-3} a_j e_j,$$

where a_j is the ionic charge. This is not an easy sum to evaluate because it is only slowly convergent. The number of charges in a shell goes as r^2 and their effect as r^{-3} , so that the effect of larger and larger shells falls only as r^{-1} . Convergence results only because the larger shells contain more nearly equal numbers of positive and negative ions more nearly uniformly distributed over the spherical shell. A much more rapidly convergent sum can be obtained if the configuration can be expressed as a small distortion from a cubic or other

symmetry in which q is known to be zero. Little seems to be known about the shielding effect of the ion of the subject nucleus, but determinations of spectra in crystals containing nuclei of known Q would yield information on this point. Unfortunately, the Al_2O_3 crystal appears to be strongly molecular and does not serve as a test in this respect. The value of q in this crystal, using $Q = 0.15 \pm 0.003 \times 10^{-24} \text{ cm}^2$ as determined by Lew³⁷ is $\pm 4.66 \pm 0.12 \times 10^{23} \text{ cm}^{-3}$. More quantitative data on relaxation times in cubic alkali halide crystals might show whether this effect could be utilized for the rough determination of electric quadrupole moments.

One quantity that is most unambiguously determined from spectra of this kind is the nuclear spin. The principal difficulty in applying this technique for the determination of spins is that of finding suitable single crystals. As an example, some effort has been made to obtain crystals in which the spins of B^{10} and B^{11} could be observed from the structure of their magnetic resonance spectra. Natural crystals containing boron are

³⁷ H. Lew, Phys. Rev. **76**, 1089 (1949).

mostly boro-silicates and are very diluted as samples of boron and, in addition, contain several boron atoms in non-equivalent positions in a unit cell. Borax and similar compounds form crystals containing many water molecules, resulting in dilution of the sample and consequently weak lines. So far a satisfactory crystal has not been obtained. Both the B^{11} and the Na^{23} lines in a single crystal of $\text{Na}_2\text{B}_4\text{O}_7 \cdot 5\text{H}_2\text{O}$ have been found to show structure that depends on orientation but it is not yet understood.

The author would like to express gratitude for the interest and encouragement of many of his colleagues in the Lyman Laboratory, especially that of Professor E. M. Purcell. The form of the presentation in the theoretical section has benefited greatly from the work of Dr. R. Bersohn³⁸ who has treated these and other aspects of the electric quadrupole interaction in solids. Support of a large part of this research by the Society of Fellows at Harvard University is gratefully acknowledged.

³⁸ R. Bersohn, Thesis, Harvard University (1950).

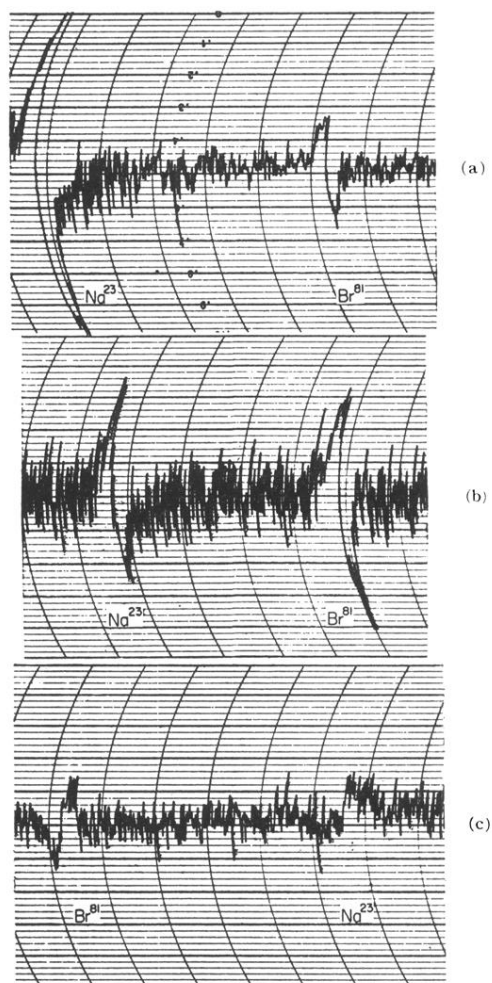


FIG. 12. The Na^{23} and Br^{81} resonances in NaBr show different relaxation times. In (a) and r-f signal level of 0.12 volt is used, in (b) about 0.5 volt, and in (c) about 1 volt across the r-f coil. The tuning capacity was about $150 \mu\mu\text{f}$ and with the coil volume of about 5 cc the resulting magnitudes of the rotating magnetic field H_1 are 0.005, 0.02, and 0.04 gauss, respectively.

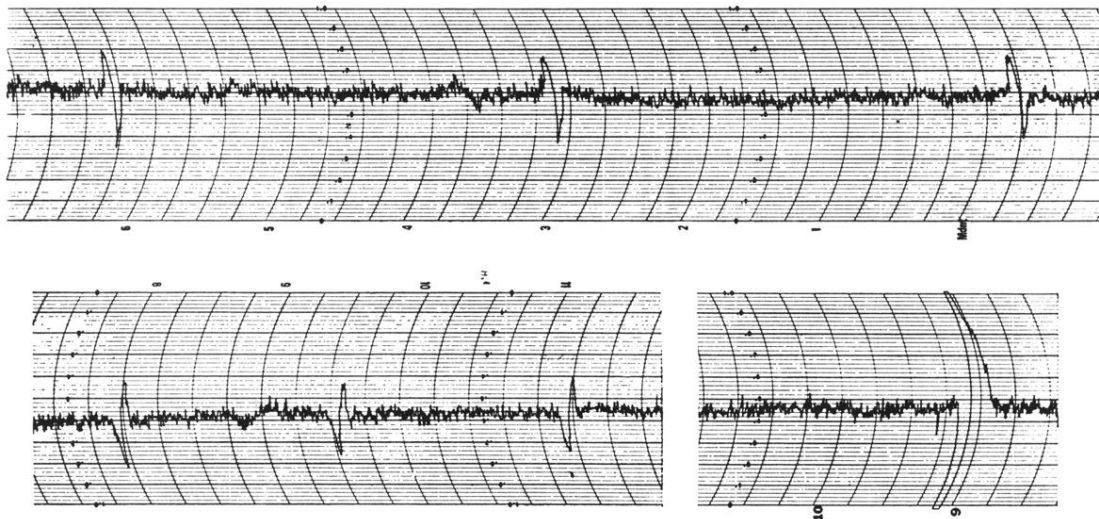


FIG. 5. The Na^{23} resonance in NaNO_3 for crystal axis near 0° , 90° , and 54° with respect to H_0 . The frequency scale is about 14 kc per division, which corresponds to 15 minutes of time. The frequency of the center line is 7.18 Mc. A small effect explainable through higher order terms in the perturbation can be seen to cause an asymmetry in the line at $\theta = 54^\circ$.

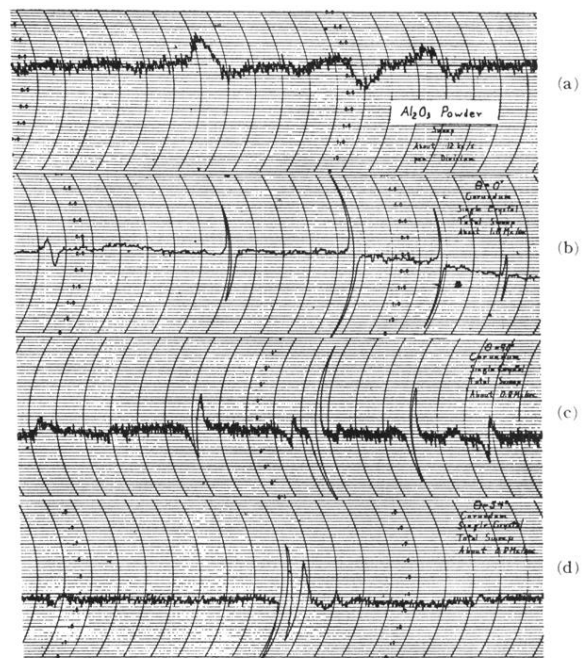


FIG. 7. Spectra of Al^{27} in Al_2O_3 . (a) A powder pattern near 3 Mc with total sweep about 900 kc. (b) A single crystal with hexagonal axis parallel to H_0 . The total sweep is about 1.6 Mc centered at 3 Mc. The 20-sec. time constant is used here. (c) With the crystal axis perpendicular to H_0 , the sweep rate about doubled and the 1-sec. time constant used. (d) With crystal axis at 54° to H_0 , same sweep rate and time constant as in (c).